Lawrence Berkeley National Laboratory
Recent Work

Title

THE ^NCp^t)1^ AND ""^(p^e)1^ REACTIONS AND THE SPECTROSCOPY OF LEVELS IN MASS 13

Permalink

https://escholarship.org/uc/item/5dd988wp

Authors

Fleming, Donald G.
Cerny, Joseph
Maples, Creve C.
et al.

Publication Date

1967-09-01

$e\cdot 2$

University of California

Ernest O. Lawrence
Radiation Laboratory

THE ^{15}N(p, t) ^{13}N AND ^{15}N(p, ^{3}He) ^{13}C REACTIONS AND THE
SPECTROSCOPY OF LEVELS IN MASS 13

Donald G. Fleming, Joseph Cerny, Creve C. Maples
and Norman K. Glendenning

September 1967

DISCLAIMER

UNIVERSITY OF CALIFORNIA

Lawrence Radiation Laboratory
Berkeley, California

AEC Contract No. W-7405-eng-48

THE ^{15}N$(p,t)^{13}$N AND ^{15}N$(p,^3$He$)^{13}$C REACTIONS AND THE SPECTROSCOPY OF LEVELS IN MASS 13

Donald G. Fleming, Joseph Cerny, Creve C. Maples
and Norman K. Glendenning

September 1967

THE ^{15}N(p,t)^{13}N AND ^{15}N(p,^{3}He)^{13}C REACTIONS AND THE SPECTROSCOPY OF LEVELS IN MASS 13

Donald G. Fleming,[†] Joseph Cerny, Creve C. Maples
and Norman K. Glendenning

Lawrence Radiation Laboratory and
Department of Chemistry
University of California
Berkeley, California

September 1967

A 43.7 MeV proton beam has been used to induce (p,t) and (p,^{3}He) reactions on an ^{15}N target. Transitions to mirror final states of ^{13}N and ^{13}C have been investigated over 15 MeV of excitation and several new spin and parity assignments have been made. The DWBA predictions of angular distributions for these ^{15}N(p,t)^{13}N and ^{15}N(p,^{3}He)^{13}C reactions, using intermediate coupling wave functions to obtain the two-nucleon structure factors, were generally found to reproduce experiment well; in addition, calculated cross sections for the ^{15}N(p,t)^{13}N reaction were in good agreement with the experimental values.

[†]Now at the Nuclear Structure Laboratory, University of Rochester, New York.

I. INTRODUCTION

It is the purpose of this paper to discuss the nuclear spectroscopy of

the mass 13 nuclei from a comparison of the $^{15}N(p,t)^{13}N$ and $^{15}N(p,^{3}He)^{13}C$ reac-

tions populating mirror final states. In the past, work at this laboratory

has shown that comparisons of (p,t) and $(p,^{3}He)$ transitions are valuable spectro-

scopic tools for identifying and characterizing isobaric analogue states.[1]

However, because analogue states were of interest, little work on comparisons

of these reactions to other final states, except for that presented in Ref. 2,

has been previously reported. For the data discussed herein, such comparisons

permit several new spectroscopic assignments to be made.

In the following we attempt to fit both the shapes and the magnitudes

of these (p,t) and $(p,^{3}He)$ transitions with distorted wave Born approximation

(DWBA) calculations,[3,4] thereby testing the mass 13 wave functions of Cohen and

Kurath[5] over 15 MeV of excitation. Although many examples of two-nucleon DWBA

fits to individual transitions exist in the literature, only recently[6-9] has much

attention been paid to the more comprehensive problem of fitting both the shapes

and the relative magnitudes of two-nucleon transitions. This report is the

first time that such calculations have been extended to cover a wide range of

excitation.

II. THEORY

The formulation of the theory of direct two-nucleon transfer reactions by most authors[3,4,10] is essentially equivalent. (An exception is the work of Rook et al.[11] who, in addition to the zero-range interaction employed by others, also use a point triton approximation). However, the formulation of Ref. 4 was made with particular emphasis on the role played by the structure of nuclear states in the reaction and will be used throughout this analysis. This theory fully takes into account the coherent effects caused by the spatial and spin correlations between the nucleons in the picked-up pair, which are expressed in the shell model by configuration mixtures.

For details of the theory, the reader is referred to Ref. 4. Here we briefly recapitulate the main ingredients involved in a calculation of two-nucleon transfer reactions. The lowest order transfer does not entail any re-arrangement of nucleons other than those removed from the target and this establishes the _parentage_ of the states that can be excited. Further, because the nucleons are transferred to or from a light nuclide having simple and presumably known[12] _spatial and spin correlations,_ a nuclear state is excited only to the extent that these pair correlations are present.[4] This informa-tion is conveniently incorporated into a calculation of the cross section through the function which describes the center-of-mass motion of the trans-ferred pair, when they are appropriately correlated and when the nuclear state has the required parentage. Then, in the DWBA treatment,

a   calculation of the cross section involves evaluation of the usual type of integrals[3,4] involved in all direct reactions, with the above described center-of-mass wave function entering as the "form factor".

Since most nuclear structure calculations employ harmonic-oscillator functions (in any case, all single-particle wave functions can be expanded in terms of them), the projected center-of-mass wave function for the two-nucleon transfer reaction can be written as

$$\tilde{U}_L(R) = \sum_N G_{NLSJT} \, U_{NL}(2\nu R^2)$$

where U_{NL} is a harmonic oscillator function and $\nu = m\omega/\hbar$ is a constant corresponding to the particular single-particle motions involved. Because of the poor asymptotic behavior of the oscillator functions, $\tilde{U}_L(R)$ is matched (at the nuclear surface) to the appropriate Hankel function with asymptotic behavior corresponding to the separation energy of the pair.

The structure amplitudes G_{NLSJT} are calculated from the wave functions used to describe the initial and final nuclear states. They carry all the nuclear structure information relevant to the reaction and their explicit form was given previously.[4] Generally, they involve a sum over several configurations of the pair since this is the way in which correlations are expressed in the shell model.

One of the factors involved in the calculation of the structure amplitude G_{NLSJT} is the parentage factor $\beta[(j_1 j_2)_J]$ that measure the degree to which the state of the nucleus (A+2) has as its parent the nucleus (A), with the transferred pair in the state $(j_1 j_2)_J$. Using the general definition of Ref. 4, the parentage factors for several types of configurations[5] excited in the $^{15}N(p,t)^{13}N$ and $^{15}N(p,^{3}He)^{13}C$ reactions[13] are now given (a neutron-proton formalism is used).

The target wave function has spin j and is written as

$$|\psi_T\rangle = |(j_a^{n_a})_0 (j_b^{n_b})_0, j;j\rangle$$

1) for a pair of like nucleons added or taken out of a given shell — say j_b — where n_b is even, the final state wave function has the form

$$|\psi_F\rangle = |(j_a^{n_a})_0, (j_b^{n_b-2})_J, j;J_f\rangle$$

The parentage factor relating initial and final state configurations for a particular total angular momentum transfer J and a particular final state spin J_f is

$$\beta[(j_b)_J^2] = \left(\frac{n_b(n_b-1)}{2}\right)^{1/2} ((j_b^{n_b-2})_{vJ} (j_b^2)_J; 0|\} (j_b^{n_b})_0) \left(\frac{2J_f+1}{(2J+1)(2j+1)}\right)^{1/2}$$

Explicit expressions for the two-nucleon coefficients of fractional parentage ($|\}$) may be found in Ref. 4 or Ref. 14.

2) for a pair of nucleons transferred across shells or a pair of non-identical nucleons (a neutron-proton pair) transferred within the same shell, the final state wave function has the form

$$|\psi_F\rangle = |[(j_a^{n_a-1})_{j_a} (j_b^{n_b-1})_{j_b}]_J, j;J_f\rangle$$

where the square bracket denotes vector coupling and n_a and n_b are even. The parentage factor relating this configuration to the initial state by the total angular momentum transfer J is given by

$$\beta[(j_a,j_b)]_J = (n_a n_b)^{1/2} \left(\frac{2J_f+1}{(2j_a+1)(2j_b+1)(2j+1)} \right)^{1/2}$$

The DWBA calculation[4] involves use of these parentage factors in LS coupling and this is achieved by the appropriate jj-LS transformation coefficient. The calculation for states of mixed configuration[5] involves the appropriate linear combination of the above β's. Explicit derivations of these expressions are given in Ref. 15.

II. EXPERIMENTAL

These reactions were induced by a 43.7 MeV proton beam from the Berkeley spiral ridge cyclotron. The physical layout of the cyclotron and target area, together with the overall beam optics, is illustrated in Fig. 1. In the radial plane, the first set of quadrupole magnets (Quad. 1) creates an image of the virtual source just prior to the entrance of the switching magnet. The beam is then deflected 38° by the switching magnet through a second set of quadrupole magnets (Quad. 3) which produces a radial focus at the analyzing slit. For our experiments, this slit consisted of two vertical tantalum plates, 125 mils thick, and normally set 60 mils apart. In the vertical plane, only one focus is required prior to the scattering chamber. This occurs at the exit of the switching magnet. Beyond the analyzing slit, two quadrupole lens doublets (Quad. 21, Quad. 22) were required to bring the beam to a radial and vertical focus at the center of a 20" diameter scatter chamber. Typical beam spot sizes at this point were 80 mils wide × 100 mils high, with beam intensities varying between 0.05 and 1.0 μa, as required. The beam current was measured in a Faraday cup with an integrating electrometer.

Reaction events were measured in two separate counter telescopes, each consisting of a 5.5 mil phosphorus-diffused silicon ΔE detector and a 120 mil lithium-drift silicon E detector, backed by a 20 mil lithium-drift silicon detector. This last counter served to eliminate signals from long range events which passed through the first detectors. The target was 99% pure $^{15}N_2$ gas and was contained in a three inch diameter gas cell which was filled externally. A 315° gas target window was covered with 0.1 mil Haver foil[16] which easily withstood pressures of 30 cm of mercury. The target pressure and beam energy were constantly monitored by a 120 mil lithium-drift silicon detector fixed at 27.5° to the beam.

A block diagram of the electronics is shown in Fig. 2. Signals from the three detectors (ΔE, E, $E_{rej.}$) were first sent to charge-sensitive pre-amplifiers which then fed the main amplifiers in the circuit. ΔE and E signals from these amplifiers were then fed to a Goulding-Landis particle identi-fier.[17] This unit operates on the empirical relation $R = aE^{1.73}$, where R is the range of the particle, E is its total energy and a is a constant, char-acteristic of the particle type. A particle identifier spectrum is shown in Fig. 3. Particle identifier signals were selectively gated in a 4-channel router so that valid triton, helium-3 (and alpha particle) events could be recorded in the appropriate channel of a Nuclear Data analyzer or in an on-line PDP-5 computer, both operating in a 4×1024 channel mode. Since it was not always possible to completely separate deuterons and tritons with this relatively thin ΔE detector, a safety group was observed in which any leak-through tritons were collected. Energy resolutions (FWHM) of 150 and 180 keV were obtained for tritons and helium-3, respectively.

III. RESULTS

Figure 4 presents energy spectra of the $^{15}N(p,t)^{13}N$ and $^{15}N(p,^3He)^{13}C$ reactions taken at 15° in the laboratory. The excitations shown were obtained in this experiment and for the most part agree with previous values,[18] as shown in Tables I and II. Those levels marked with an asterisk in these tables were used to determine the energy scale and their associated errors (in keV) reflect the overall uncertainties involved in the analysis. In addition, spin and parity assignments are presented in these tables, and these will be fully explained later in the text. An energy level diagram for ^{13}C and ^{13}N is presented in Fig. 5. The data in Fig. 4 show that the reaction is very selective, strongly populating only the negative parity states in the mass 13 nuclei. This is expected on the basis of a direct pickup of two nucleons from a $(1p)^{11}$ configuration, which is assumed for the ground state of ^{15}N. However, some positive parity levels are excited relatively strongly and their presence in the spectra will also be discussed. Figure 6 presents energy spectra for the $^{14}N(^3He,\alpha)^{13}N$ and $^{14}N(d,^3He)^{13}C$ reactions[19] taken at a laboratory angle of 17°, which will be used to support some of the later discussion. Similar data on single-nucleon transfer reactions populating states in ^{13}N have been obtained in recent $^{14}N(p,d)^{13}N$ experiments.[20]

Angular distributions for levels excited in the $^{15}N(p,t)^{13}N$ and $^{15}N(p,^3He)^{13}C$ reactions are shown in Figs. 7-12; the statistical errors are contained within the points unless explicitly indicated. The total integrated cross sections for these reactions are presented in Tables I and II; the absolute errors on the large transitions are expected to be $\leq$ 10 percent. Representative relative errors for all states are given in these tables. Of later interest will be Fig. 13 and Fig. 14 which present (p,t) L=0 and L=2

angular distributions obtained on a variety of light nuclei. These are remark-
ably similar in shape, considering the range of particle energies involved.
Hintz and co-workers[21] have observed similar effects in (p,t) reactions on
heavier nuclei.

IV. DISCUSSION

We wish to analyze the negative parity levels excited in the $^{15}N(p,t)^{13}N$
and $^{15}N(p,^{3}He)^{13}C$ reactions. The energy levels observed are compared with
those predicted by intermediate coupling theories and the experimental angular
distributions are compared with the two-nucleon transfer theory of Ref. 4.
Later, the performance of this theory in predicting relative cross sections for
these transitions is noted. However, prior to these analyses the optical model
parameters used in this study require discussion:

Since appropriate elastic scattering data were not available in either
the entrance or the exit channel, the optical model parameters were obtained
from an examination of the "best fit" parameters available in the literature.
There are only a few reports of about 40 MeV proton scattering on light nuclei
(see, for example, Refs. 22 and 23) and, unlike what is available in our code,
most of these fits[22] have employed a spin-orbit term in the optical potential.
However, we are able to employ a real well depth which is consistent with the
values given in Refs. 22 and 23, though the absorptive potential had to be in-
creased considerably. The proton potential that proved to give the best over-
all fit to the data was interpolated from a graph of optical model parameters
vs. energy, given by Bjorklund.[24]

The choice of an exit channel potential -- in the absence of elastic
scattering data -- is perhaps subject to the most uncertainty. In accord with

the hypothesis that in a reaction involving complex particles one should con-
sider the interaction of each nucleon with the scattering center,[25,26] we have
used triton and helium-3 optical model parameters corresponding to a sum of
single-nucleon potentials. These were obtained from searching the literature
for the appropriate low energy (about 10 MeV) nucleon scattering data on light
nuclei.[27] Parameters obtained in this way are similar to those found from
helium-3 optical model fits on light nuclei[28] in the energy region of our
experiment (about 25 MeV), although this reference generally employed larger
radii for the imaginary well. (There are no optical model parameters available
for triton scattering on light nuclei at these energies). The best "summed"
potential was determined from the ^{15}N(p,t)^{13}N data alone since only a single
L transfer was allowed in these transitions and this potential is presented
in Table III (potential X) along with the proton potential[24] mentioned above
(potential A). The exit channel parameters were taken to be the same for both
tritons and helium-3 and are labeled just by the triton channel in Table III.
Earlier work in fitting helium-3 elastic scattering data on light nuclei[29]
employed a "shallow" potential for the real well depth and an average of the
parameters given in Ref. 29 is shown in Table III (potential Y). In addition,
Table III contains a potential found[8] from 30 MeV helium-3 scattering on ^{12}C
(potential Z). The combination that produced the best overall results -- over
15 MeV of excitation -- was AX. Although the proton potential was relatively
insensitive to the choice of volume or surface (derivative Saxon-Wood) absorption,
the triton potential in the AX combination gave better overall fits to the data
with surface absorption.

DWBA fits to the data are compared in Fig. 15 and Fig. 16 for the $^{15}N(p,t)^{13}N$ ground state (L=0) and $^{15}N(p,t)^{13}N$ 7.38 MeV (L=2) transitions, respectively, utilizing the potentials AX, AY, and AZ of Table III. The fits have all been arbitrarily normalized to the data,at 32° for the ground state transition (Fig. 15) and at 20° for the 7.38 MeV transition (Fig. 16). These are the two strongest states in the spectrum, so that they should be good tests for the correctness of the optical model wave functions. The ground state transition (L=0) is best fit with potential AZ while the 7.38 MeV transition (L=2) is best fit with potential AX. However, AX generally fits the other transitions in the (p,t) data better than AZ does. For both transitions, the "shallow" potential AY gives a relatively poor fit to the data. All of the (p,t) and $(p,^{3}He)$ fits discussed in the following have been calculated with the potential AX. Attempts to improve the DWBA fits to excited states thru introducing an energy dependence in the triton potential by reducing the real well depth as a linear function of excitation[24,30] were not successful; the DWBA results continued to look better with the AX potential fixed for all excited states.

A. Spectroscopy of Individual Levels

Considerable theoretical interest has been concentrated on nuclei in the lp shell within the framework of the intermediate coupling model. The early calculations of Inglis[31] and Lane[32] were followed by those of Kurath,[33] Boyarkina[34] and Barker.[35] In all of these calculations the nucleon-nucleon interaction was taken to be purely central and the ratio "a/k", where "a" is the strength of the spin-orbit potential and "k" is the value of the two-body

exchange integral, was left as a variable parameter. More recently Halbert et al.[36] reported a calculation similar to those above but using the Hamada-Johnston potential[37] for the nucleon-nucleon interaction, rather than a simple central interaction. An alternative approach is the "effective interaction" treatment of the problem, where the nucleon-nucleon potential is not explicitly defined and the matrix elements of the two-body interaction are left as parameters to be determined by experiment. Calculations of this kind have recently been reported by Cohen and Kurath[5] and Barker.[38] In Table IV, which will be referred to in the following discussion, are shown the predictions of these calculations (Refs. 5, 33-36) for the levels in mass 13, along with the experimental assignments.

As mentioned earlier, the two-nucleon transfer theory[4] requires a separate calculation of the nuclear structure factors (G_{NLSJT}) which are then used in the DWBA calculation. These factors have been calculated using coefficients of fractional parentage derived from Cohen and Kurath's complete intermediate coupling wave functions[5] and are presented in Table V (multiplied by the spin-isospin coupling factor, C_{ST}).[4] Harmonic oscillator wave functions are assumed for the single particle states in the nuclear structure calculation and the oscillator parameter v is taken to be 0.32 F^{-2}, which is the same value that True employed for the lp levels in his shell model calculation of ^{14}N.[39]

The individual transitions are now discussed:

1. O MeV, [^{13}N and ^{13}C], 1/2$^-$

Two nucleon transfer selection rules restrict this transition to a pure L=0 transfer for the (p,t) reaction but allow both L=0 and L=2 for the (p,^{3}He) reaction. The DWBA fits are shown in Fig. 17 and are arbitrarily normalized --

the (p,t) independently of the (p,^{3}He). The theoretical (p,t) cross section
is overpredicted at back angles but otherwise gives a reasonably good account
of the data. The (p,^{3}He) fit, which gives a good representation of the envelope
of the angular distribution, does not completely account for the forward angle
behavior of the data. A better fit can be obtained through the inclusion of
a strongly spin-dependent force, which is later referred to and which enhances
the L=0 component of this transition.

2. $\underline{3.51 \text{ MeV } [^{13}N] \text{ and } 3.68 \text{ MeV } [^{13}C], \ 3/2^-}$

Two-nucleon transfer selection rules now restrict the (p,t) transition
to be pure L=2 while the (p,^{3}He) is again a mixture of L=0 and L=2. The DWBA
fits to these data,[40] normalized separately and independently of the ground
state transition, are shown in Fig. 18. The (p,t) transition is well predicted
by the theory; the (p,^{3}He) fit does not completely reproduce the back angle
structure, although it gives a good account of the forward angle behavior.

3. $\underline{7.38 \text{ MeV } [^{13}N] \text{ and } 7.55 \text{ MeV } [^{13}C], \ 5/2^-}$

Early ^{12}C + proton scattering results by Shute et al.[41] indicated that
the parity of this level (in ^{13}N) should be positive ($5/2^+$, $7/2^+$), in agreement
with the results of other workers.[42] Barker,[43] from an analysis of some
^{12}C(p,p'γ) results, agreed that the spin of the level was either 5/2 or 7/2,
but of negative parity. Based on the results of his intermediate coupling
calculations,[35] which are reproduced in Table IV, Barker assigned this level
as $5/2^-$. Similar calculations by both Kurath[33] and Boyarkina[34] predicted a
$5/2^-$ level at about 6 MeV of excitation (Table IV); further, Gallman et al.[44]
show that a value of about 3.5 for a/k, in good agreement with Barker's
choice, is required in order to predict a $5/2^-$ level at about 7 MeV of excitation.

Nevertheless, recent $^{12}C(p,p'\gamma)$ experimental results[45] could not clearly distinguish between a 5/2⁻ or a 7/2⁻ assignment.

Transitions to this level are the strongest ones in the $^{15}N(p,t)^{13}N$ spectra. They show a characteristic L=2 angular distribution (compare Figs. 13 and 14) which requires either a 3/2⁻ or a 5/2⁻ assignment, and 3/2⁻ seems unlikely in view of the evidence presented above. From this and the relative cross section results discussed later, we are able to confirm that the level in question is 5/2⁻, a conclusion which has also been reached from recent $^{14}N(p,d)^{13}N$ analyses.[20] The mirror level is observed at 7.55 MeV in ^{13}C via the $(p,^3He)$ reaction. Unlike the ground state and first excited states, however, the $(p,^3He)$ transition is now restricted by angular momentum coupling to a pure L=2 transfer. Consequently, these (p,t) and $(p,^3He)$ 5/2⁻ transitions are expected to have similar angular distributions. The DWBA fits for these transitions are shown in Fig. 19. The theory gives a very good account of the shape of the (p,t) angular distribution and a reasonable fit to the $(p,^3He)$ data, although it has not been able to account for the shift of the first maximum toward smaller angles observed in the $(p,^3He)$ angular distribution. Nevertheless, its angular distribution is well enough characterized to confirm a 5/2⁻ assignment for the 7.55 MeV level in ^{13}C.

4. <u>8.93 MeV [^{13}N] and 8.86 [^{13}C], 1/2⁻</u>

This level has been strongly excited in ^{13}N via proton scattering on ^{12}C by a p-wave resonance[41] and a spin-parity of 1/2⁻ has been assigned. It is also strongly excited in the $^{14}N(^3He,\alpha)^{13}N$ reaction (Fig. 6) and the $^{14}N(p,d)^{13}N$ reaction.[20] The analysis of the 8.93 MeV level observed in the $^{15}N(p,t)^{13}N$ reaction (its width is known[18] to be 230 keV) yields a reasonable

L=0 angular distribution (Fig. 7), in agreement with its 1/2⁻ assignment. A level at 8.86 MeV in ^{13}C, which is probably the mirror of the 8.93 MeV level in ^{13}N, is populated in the ^{15}N(p,^{3}He)^{13}C reaction. It has an angular distribution fairly similar to the (p,t) transition,which is understandable on the basis of the nuclear structure calculations; as indicated in Table V, the L=0 strength in the (p,^{3}He) cross section is expected to be about a factor of three stronger than the L=2 strength. As expected, a level at this excitation (8.8 MeV) is also strongly excited in the ^{14}N(d,^{3}He)^{13}C reaction (Fig. 6). Intermediate coupling predictions for the appearance of a second 1/2⁻ level in this energy region are generally in very good agreement with experiment (see Table IV).

The DWBA predictions for the angular distributions to these levels are shown in Fig. 20, again normalized independently. These fits are of poor quality compared to the ones previously presented. In addition (see Sec. IV-B), the relative cross section for this 8.93 MeV 1/2⁻ transition is underpredicted in the DWBA calculation by a factor of 600, whereas agreement to within a factor of two is obtained for all the other (p,t) transitions. However, the cross sections predicted from ^{14}N(^{3}He,α)^{13}N and ^{14}N(p,d)^{13}N DWBA analysis[19,20] for this level agree with experiment to better than a factor of two. This enormous discrepancy in the (p,t) reaction is difficult to understand and will be discussed later.

5. **9.48 MeV [^{13}N], 3/2⁻ and 9.52 MeV [^{13}C], (3/2⁻)**

This level was originally assigned 3/2⁻ in ^{13}N from proton scattering results[41] on ^{12}C and until recently was thought to correspond to the second 3/2⁻ level predicted by intermediate coupling theory (Table IV). However, it is virtually absent in the ^{15}N(p,t)^{13}N spectra and it is not observed in the ^{14}N(p,d)^{13}N or ^{14}N(^{3}He,α)^{13}N reactions (Fig. 6).[20,19] The single-nucleon pick-

up data are particularly interesting since coefficients of fractional parentage for these reactions[5] show that a second 3/2⁻ level, predicted to lie at about 10 MeV of excitation, should be strongly populated. Furthermore, the structure factors shown in Table V from the Cohen and Kurath work[5] indicate that the second 3/2⁻ level populated in the (p,t) reaction should be roughly only a factor of five weaker than the first 3/2⁻ level (3.51 MeV). This would imply a peak angle cross section of about 80 μb and thus should be as strong as the T=3/2 level (15.07 MeV, 3/2⁻), which is clearly seen in the spectrum (Fig. 4). The evidence presented here, then, seems to indicate overwhelmingly that the 9.48 MeV 3/2⁻ level in ^{13}N is not primarily composed of a $(1p)^9$ configuration, and is therefore not the second 3/2⁻ level predicted by intermediate coupling theory. This interpretation is supported further by the data of McPherson et al.,[46] who studied the beta decay of ^{13}O. The log ft values for this decay (and also for the beta decay of the mirror ^{13}B nucleus)[47] are in good agreement with intermediate coupling calculations,[5] except for the transition to the 9.48 MeV 3/2⁻ level in ^{13}N. In fact, it is possible that this particular level contains appreciable $(2s,1d)^2$ admixtures.[5] Such configurations could not be excited in the beta decay of ^{13}O and would not be appreciably excited in these nuclear reactions. The second 3/2⁻ level predicted by theory is found to lie at 11.9 MeV as discussed below.

However, a level at 9.52 MeV is excited in the ^{15}N(p,^{3}He)^{13}C reaction, which is relatively strong in comparison to the other levels in this region (Fig. 4 and Table II). A level at this excitation has also been observed in the ^{14}N(d,^{3}He)^{13}C reaction (Fig. 6) which, although weakly populated, is excited stronger than any of the positive parity levels of ^{13}C. This is a good

indication that the 9.52 MeV level in ^{13}C is of negative parity and one might

consider it to be the 3/2$^-$ mirror of the 9.48 MeV 3/2$^-$ level in ^{13}N.[18] The

angular distribution seems to be predominantly L=2 (compare Figs. 12, 13 and 14)

which is consistent with a 3/2$^-$ assignment. However, a puzzling aspect about

this (p,^{3}He) transition is its appreciable cross section (Table II), especially

relative to the missing mirror (p,t) transition. Both of these levels -- the

9.48 MeV in ^{13}N and the 9.52 MeV in ^{13}C -- can be expected to mix with

neighboring 3/2$^-$ levels, the nearest being the 11.90 MeV level, which is dis-

cussed below. This last level has strong components of quartet spin states[34]

which would be "S forbidden" in the (p,t) reaction (see Ref. 2). Such com-

ponents mixed into the 9.5 MeV 3/2$^-$ level could favor the (p,^{3}He) transition.

6. 10.78 MeV [^{13}N], 1/2$^-$, and 11.09 MeV [^{13}C], (1/2$^-$)

A new state in the ^{13}N spectrum possessing a small cross section (less

than that to the 6.38 MeV 5/2$^+$ level) is observed at 10.78 MeV; tritons from

this level show an angular distribution sharply peaked forward at small angles

(Fig. 7). A level at this excitation is also weakly excited in the

^{14}N(^{3}He,α)^{13}N reaction (Fig. 6) although here it is much more strongly popu-

lated than any of the positive parity levels. The relative strength with which

the 10.78 MeV level is populated in the (^{3}He,α) reaction indicates a level of

negative parity and its L=0 angular distribution (compare Figs. 13 and 14) in

the (p,t) reaction (albeit with very poor statistics) indicates a probable spin

and parity of 1/2$^-$.

In contrast to the (p,t) data, the (p,^{3}He) transition to a level at

11.09 MeV in ^{13}C, which is probably the mirror of the one above, is more strongly

populated. Although only a few angles were taken, the ^{14}N(d,^{3}He)^{13}C reaction

(Fig. 6) excites a level at 11.1 MeV, in good agreement with this value. There are two known[18] levels in this region of ^{13}C, at 11.01 and 11.08 MeV, and it would appear from our energy analysis that the second one is populated in the ^{15}N(p,^{3}He)^{13}C reaction. (The level at 11.01 MeV has been tentatively assigned as 1/2$^+$, which one would not expect to be appreciably excited).

The angular distribution of this ^{15}N(p,^{3}He)^{13}C transition is presented in Fig. 11 and indicates a mixture of L=0 and L=2 transfers, which would be consistent with either a 1/2$^-$ or a 3/2$^-$ assignment. Assuming that the 10.78 MeV level in ^{13}N and the 11.09 MeV level in ^{13}C correspond to the third 1/2$^-$ state predicted by theory (Table IV) produced the DWBA fits shown in Fig. 21. The L=0 shape for the (p,t) transition is well reproduced over the peak and, as we later discuss, the relative cross section of this level is in much better agreement for this choice than with a 3/2$^-$ (L=2) assignment. The (p,^{3}He) angular distribution is also reasonably well fit for a level at this high excitation. An assignment of 1/2$^-$ is consistent with the above fits and a complete DWBA analysis of the ^{14}N(^{3}He,α)^{13}N data[19] confirms this conclusion.

7. <u>11.88 MeV [^{13}N], 3/2$^-$, and 11.80 MeV [^{13}C], (3/2$^-$)</u>

This level in ^{13}N has been recently observed in single-nucleon transfer reactions on ^{14}N [19,20] (Fig. 5) through a p 3/2 neutron pickup. An analysis of the intermediate coupling wave functions for the various final states[5] shows that the 5/2$^-$, 7.38 MeV level; the 1/2$^-$, 8.93 MeV level; and a 3/2$^-$ level should all have the same dominant configuration, $|(p_{1/2})^2_1, (p_{3/2})^{-1}; J\rangle$, and consequently these would all be expected to be strongly excited in single-nucleon transfer reactions on ^{14}N. All three are indeed strongly excited, in good agreement with Cohen and Kurath's spectroscopic factors,[5] and on this

basis a $3/2^-$ assignment[20] was made for the level at about 11.9 MeV in ^{13}N. A

level at 11.88 MeV has been observed in the ^{15}N(p,t)^{13}N reaction and one at

11.80 MeV in the ^{15}N(p,^{3}He)^{13}C reaction—this latter level most likely being

the mirror of the one in ^{13}N. This ^{13}C level has also been observed in

^{14}N(d,^{3}He)^{13}C (Fig. 6) and ^{13}C(^{3}He,^{3}He')^{13}C reactions.[19] The (p,t) reaction

populating a $3/2^-$ level is restricted by two-nucleon transfer selection rules

to a pure L=2 transfer and the angular distribution of the 11.88 MeV transition

is shown in Fig. 8. The (p,^{3}He) transition, on the other hand, can be populated

by both L=0 and L=2 components and its angular distribution is given in Fig. 11.

The DWBA fits for these levels, using intermediate coupling wave

functions for the second predicted $3/2^-$ level, are given in Fig. 22. For the

(p,t) transition, both a representative L=0 transition at this excitation and

an L=2 transition are compared with the data. It can be seen that L=2 gives a some-

what better overall fit, which is consistent with the $3/2^-$ assignment. The

DWBA calculation is, however, unable to account for the small angle behavior

observed. This shift of the most forward experimental maximum to smaller angles with

increasing excitation has been observed in other (p,t) transitions (Figs. 13

and 14). The theory, on the other hand, exhibits a slight shift outward

in angle with increasing excitation. The ^{15}N(p,t)^{13}N 7.38 MeV (L=2) transition

gave a slight indication of this effect, although not so drastic as observed

here. The (p,^{3}He) fit, on the other hand, is quite good, especially for

such a highly excited state. Both the structure and the envelope of the cross

section are well predicted by the theory, which gives a good indication for

a $3/2^-$ assignment to the 11.80 MeV level in ^{13}C.

8. __12.40 MeV [^{13}C], 7/2$^-$__

A level at 12.40 MeV in ^{13}C was excited fairly strongly in the ^{15}N(p,^{3}He)^{13}C reaction, although its counterpart in the ^{15}N(p,t)^{13}N spectra was completely absent. A previously reported level at 12.44 MeV excitation[18] in ^{13}C has been tentatively assigned as 1/2$^-$. This level at 12.40 MeV had a width consistent with the recently reported value of 90 keV,[48] in contrast with other reports on the width of a level at this excitation of about 300 keV.[49] Other levels are also observed in this region in the ^{15}N(p,^{3}He)^{13}C reaction at about 12.2 and 12.6 MeV and these could be the cause of the differing widths reported for this state. Although the 12.40 MeV level was not well resolved at most angles from these other peaks, its angular distribution was extracted and is shown in Fig. 12.

The angular distribution for this level has a reasonably pure L=2 shape at small angles (compare Figs. 13, 14) which would imply that this was a transition to a 5/2$^-$ or 7/2$^-$ final state, rather than to a 1/2$^-$ state. Intermediate coupling theory (Table IV) would argue for a 7/2$^-$ assignment. More importantly, this state is absent in the ^{15}N(p,t)^{13}N spectra and there is no evidence for a level in this range of excitation in either the ^{14}N(^{3}He,α)^{13}N or ^{14}N(d,^{3}He)^{13}C reactions (Fig. 6) or in the ^{14}N(p,d)^{13}N reaction.[20] A 7/2$^-$ assignment is the only one consistent with these observations since of the allowed 1p - shell pickup final states for this (p,^{3}He) reaction (1/2$^-$, 3/2$^-$, 5/2$^-$, 7/2$^-$) only the 7/2$^-$ state is J (or j) forbidden in all the other reactions. The DWBA fit based on a 7/2$^-$ assignment[50] (L=2) is shown in Fig. 23. The theory gives a satisfactory account of the data, predicting quite well the envelope of the cross section. For these reasons, then, the assignment of this state as 7/2$^-$ rather than the earlier 1/2$^-$ seems warranted.

9. <u>15.07 MeV [^{13}N] and 15.11 MeV [^{13}C], 3/2$^-$, T=3/2</u>

These two levels populated in the ^{15}N(p,t)^{13}N and ^{15}N(p,^{3}He)^{13}C re-

actions were reported earlier[51] and will not be discussed in any detail here.

The excitations observed are in good agreement with most intermediate coupling

calculations (Table VI), except for the results of Barker[35] which place them

almost 2 MeV too low. These are transitions from the same initial to identical

final states and as such proceed through a pure (S=0, T=1) L=2 transfer of two

nucleons for both transitions. The differential cross sections for both are

virtually the same, as shown in Figs. 8 and 12, and are discussed in more detail

in Ref. 51; the DWBA fit to the (p,t) transition is given in Fig. 23. (The

fit to the (p,^{3}He) transition was virtually the same as the (p,t) and is not

shown). The same effect observed earlier in the ^{15}N(p,t)^{13}N 11.88 MeV (3/2$^-$)

transition also appears in this (p,t) transition—namely, that the data peak

at considerably smaller angles than the theoretical fit. Nevertheless, the

DWBA fit does reproduce the observed structure and, considering that this is

such a highly excited level, is still reasonable.

10. <u>6.38 MeV [^{13}N] and 6.87 MeV [^{13}C], 5/2$^+$</u>

Insofar as the ground state of ^{15}N can be represented by a (1p)[11] con-

figuration, then the direct pickup of two nucleons can only excite negative

parity states in the final nucleus. Hence, the population of positive parity

levels must be due to other effects, such as (2s, 1d)^2 impurities in the ^{15}N

ground state or an additional mechanism such as core-excitation or knockout.

(Compound nucleus contributions are expected to be negligible at these high

bombarding energies). Only two of the experimentally resolvable positive

parity levels were consistently observed in both the (p, t) and (p, ^{3}He) spectra;

the first $1/2^+$ level at 2.37 and 3.09 MeV in ^{13}N and ^{13}C, respectively, and the second $5/2^+$ level at 6.38 and 6.87 MeV, respectively. In both spectra, the $5/2^+$ transition is much stronger and angular distributions populating it are shown in Fig. 9. Also of interest in our attempt to interpret the population of these $5/2^+$ states is the ^{13}C(p,t)^{11}C $7/2^-$ transition discussed elsewhere;[15,52] it is J-forbidden on the basis of a two-neutron pickup reaction on a pure $(1p)^9$ ^{13}C target, but is populated relatively strongly. Its angular distribution is also shown in Fig. 9. (In the following discussion, a knockout mechanism has been disregarded, in view of the relative population of the $1/2^+$ and $5/2^+$ levels and since this mechanism has been shown to be inadequate in a treatment of "j-forbidden" (d,p) reactions,[53] where its influence might even be greater than in the (p,t) reaction.)

Although the shape of the ^{13}N($5/2^+$) angular distribution is not that normally observed for an $L = 3$ transfer,[54] as would be required for pickup from a $(1d)^2$ impurity in the ^{15}N ground state, it is possible to obtain a reasonable fit to these data. In Fig. 24 are shown DWBA fits for this transition as well as for the ^{13}C(p,t)^{11}C $(7/2^-)$ transition reported previously.[15,52] Two curves are shown for each transition, corresponding to different choices for the oscillator parameter of the bound state wave function: $\nu = 0.32$ and 0.40 for the $5/2^+$ transition and $\nu = 0.32$, 0.46 for the $7/2^-$ transition. The larger values correspond to different radii for matching the Hankel function tail at the nuclear surface. (This procedure is discussed in more detail later.) Since it is not clear how to treat the bound state wave function for a (1d1p) $L = 3$ or a (1p1f) $L = 4$ transition (a problem which also arises in the analysis of single-nucleon transfer reactions[55]), these larger values of ν are perhaps not unreasonable and their use does result in improved fits to the data.

Under these assumptions and using the configurations predicted from weak coupling calculations[56] for this ^{13}N $(5/2^+)$ state, a $15 \pm 5\%$ admixture of

$(1d\ 5/2)^2$ in the ^{15}N ground state would be necessary to account for the relative strength of the observed transition. The relative population of the 6.38 MeV $5/2^+$ and 2.37 MeV $1/2^+$ levels in ^{13}N can be understood through a larger amount of $(d5/2)^2$ than of $(s1/2)^2$ in the ^{15}N ground state—a conclusion consistent with an analysis of the negative parity states populated in the $^{15}N(^3He,\alpha)^{14}N$ reaction.[57] Similar results for ^{16}O have been obtained based on the population of its 5.28 MeV $5/2^+$ level in the $^{16}O(d,^3He)^{15}N$ reaction.[28]

However, the relative population of the $1/2^+$ and $5/2^+$ levels of ^{13}N can also be understood on the basis of a core-excitation pickup reaction[58] proceeding thru the ^{15}N 5.28 MeV level.[15] Further, the observed angular distribution to the $^{13}N\ (5/2^+)$ state (and the $^{11}C\ (7/2^-)$ state) is presumably also consistent with such a mechanism. Clearly, much more theoretical work and more extensive data are required to establish the mechanism involved in populating these positive parity states.

B. Comparison of Relative Cross Sections

The discussion of relative cross sections is concentrated on the $^{15}N(p,t)^{13}N$ reaction, since a previous report[52] has shown that interference terms in the $(p,^3He)$ reaction are liable to drastically affect its cross section. Before discussing the theoretical cross sections, it is well to review how the form factor is treated in the calculation. Since the bound state wave function is represented by a harmonic oscillator, it is matched at the nuclear surface to a Hankel function tail. For a pickup reaction, the increasing separation energy of the pair with excitation has a damping effect on the magnitude of the Hankel function and this results in an increase in the matching radius with increasing excitation. For a given L transfer, this tends to cause an

increase in the predicted two-nucleon cross section with excitation, although

the magnitude of this increase can be quite sensitive to the chosen optical

model potential, as will be indicated later. An alternative method is to match

the Hankel function tail at the same radius for all excited states, which

necessitates a slight increase in the oscillator parameter ν with excitation.

Both approaches have been tried and noticeably better results are obtained with

the latter.

Relative cross sections for these two calculations are compared with

experiment in Table VI for two choices of the optical-model potential, AX and

AZ (Table III), and using the nuclear structure factors shown in Table V.

Both calculations have been arbitrarily adjusted to give the best agreement

with experiment. The calculation in which the oscillator parameter is fixed

at $\nu = 0.32$ and the matching radius is correspondingly increased gives notice-

ably poorer results for relative cross sections than the procedure adopted

whereby the matching radius is fixed (at the ground state value of 3.60f) and

the oscillator parameter adjusted. The variation in agreement of the experi-

mental and theoretical relative cross sections is indicated by the quantity B

in Table VI, which was calculated by minimizing the average value of the larger

ratio of experiment and theory for all the indicated levels and then subtracting

one from the result (B = 0 for perfect agreement). B varies from a value of

1.53 (AX potential with constant ν) to a value of 0.31 (AZ potential with

constant R = 3.60f and a 17 percent variation in ν). For both calculations,

the theoretical results using optical potential AZ are in much better agreement

with experiment than those using potential AX. Other choices were tried (including

AY of Table III) and in no case was there a significantly greater difference than

between AX and AZ. It is disappointing that potential AX shows the worst

agreement in reproducting the relative cross sections, since it gives better

overall fits to the data and is the potential used in the previous discussion.

However, potential AZ shows the best fit to the ground state transition (Fig. 15)

and also gives a reasonable fit to all the excited states (an example is shown

in Fig. 16).

The data in Table VI represent the first time, to our knowledge, that

comparisons of relative cross sections in two-nucleon transfer reactions over

15 MeV of excitation have been made. The calculation involving a fixed matching

radius for the final states must be considered as being in quite good agreement

with experiment (and is used hereafter) and insofar as our adjustment of the

oscillator parameter ν would not markedly affect the amplitudes of the inter-

mediate coupling wave functions of Cohen and Kurath,[5] then these wave functions

must be regarded as giving a good description of the final states populated in

the $^{15}N(p,t)^{13}N$ reaction.

Two points of interest appear in Table VI. First, it is important to

note that the cross section to the very weakly excited 10.78 MeV level in ^{13}N,

which we earlier assigned as $1/2^-$, is in good agreement with calculation. In

fact, assuming this level to be the next $3/2^-$ state gives a theoretical value

for the cross section (shown in brackets in Table VI) which, on the average,

is a factor of four too large. Second, of equal interest is the transition

to the 8.93 MeV $1/2^-$ state, for which the relative cross section is predicted

to be a factor of six hundred too low. However, one should note that good

agreement is obtained in the $^{14}N(p,d)^{13}N$ and $^{14}N(^3He,\alpha)^{13}N$ calculations[20,19]

for this level. We do not understand this large discrepancy; it can perhaps

be explained through coherent admixtures of other configurations or by a very

complex reaction mechanism.

Table VII presents the relative integrated cross sections for the $^{15}N(p,^3He)^{13}C$ reaction and DWBA comparisons similar to those of Table VI. The matching radius for the 3.68 MeV $(3/2^-)$ transition was held constant and the theoretical cross sections are again arbitrarily adjusted to give the best agreement with experiment. Two values of B are shown in the table, B_1 and B_2. The B_1 value arises from all the levels shown in Table VII while B_2 is calculated only for the mirror transitions corresponding to those in Table VI.

In a preceding paper[52] it was reported that the ratios of (p,t) to $(p,^3He)$ cross sections for mirror transitions were significantly improved with the introduction of a strong spin dependence in the nucleon-nucleon inter-action between the incident proton and the picked up nucleons. Since this can only affect the $(p,^3He)$ relative cross sections, calculations for both a spin-in-dependent, $A^S = A^T$, and the strongly spin-dependent interaction of Ref. 52, $A^S = 0.3A^T$, are presented in Table VII. There appears to be little difference between the spin-independent and the spin-dependent results for the B_1 calculation but the B_2 calculation shows a definite preference for the spin-independent interaction for such relative cross section comparisons. However, the previous discussion[52] of cross section ratios has shown that a spin-dependence is to be preferred, although it could not account for all the data, and one of the further suggestions made was that a coherent sum on the (LS) quantum numbers of the transferred pair in the $(p,^3He)$ reaction should be taken into account. Since the calcula-tions described above have not included this coherence, we would expect that the agreement in relative cross sections for these transitions should be signi-ficantly worse than for the mirror (p,t) transitions discussed earlier (Table VI). Comparing the two over the same range of excitation and for the same

optical potential, however, the (p,t) cross sections are found to be only in marginally better agreement with experiment. The agreement in these (p,^{3}He) cross sections is certainly acceptable -- the present theory predicting fairly well those states which are strongly or weakly excited.

It would appear from the above results that a comparison of experimental _relative_ cross sections with theory in a (p,^{3}He) [or(^{3}He,p)] reaction on a T=1/2 target does not clarify the discussion presented earlier[52] which indicated 1) a necessity for some spin-dependent nucleon-nucleon interaction in the two-nucleon transfer theory and 2) the probable necessity for including spin-orbit coupling in the optical potential. DWBA calculations that reliably predicted _absolute_ cross sections for these two-nucleon transfer reactions and could incorporate these effects would certainly resolve the problem. Insofar as the first effect is considered, a comparison of experimental and theoretical relative cross sections for (p,^{3}He), [or (^{3}He,p)] transitions on T=0 targets would be expected to be much more sensitive to the presence of a spin-dependent nucleon-nucleon force, since here the neutron-proton pair is transferred in unique ^{3}S, T=0 or ^{1}S, T=1 states. Calculations by Hardy and Towner[59] of the states populated both in the ^{12}C(^{3}He,p)^{14}N reaction at 20 MeV[8] and the ^{16}O(p,^{3}He)^{14}N reaction at 40 MeV[60] show that a spin dependence, consistent with that used in theoretical calculation and compatible with that used previously by us,[52] is required in order to account for the experimental cross sections. We will further discuss the necessity for including a spin dependence in the two-nucleon DWBA calculation in a forthcoming report on the ^{16}O(p,^{3}He)^{14}N and ^{16}O(p,t)^{14}O reactions.

Table I. Integrated cross sections of the ^{13}N levels observed in the ^{15}N(p,t)^{13}N reaction and comparison of these states with those previously reported.

	^{15}N(p,t)^{13}N		Previously Reported[18]	
	Excitation	$\sigma_T(\mu b)$		Excitation
J^π	(MeV)	(10-90°, c.m.)	J^π	(MeV)
1/2$^-$	*[a]0.0 ± 25[b]	941 ± 20	1/2$^-$	0.0
1/2$^+$	2.36 ± 30	very weak	1/2$^+$	2.366 ± 2
3/2$^-$	*3.51 ± 30	652 ± 25	3/2$^-$	3.510 ± 2
5/2$^+$	6.38 ± 30	63 ± 7	5/2$^+$	6.382
5/2$^-$	*7.38 ± 20	1271 ± 44	5/2$^-$	7.385 ± 8
1/2$^-$	8.93 ± 50	130 ± 16	1/2$^-$	8.90
	not observed		3/2$^-$	9.48
1/2$^-$	10.78 ± 60	17.6 ± 4	not reported	
3/2$^-$	11.88 ± 40	93 ± 9	3/2^{-c}	11.85
3/2$^-$	*15.07 ± 20	115 ± 11	3/2$^-$	15.068 ± 8
[T = 3/2]			[T = 3/2]	

[a]Levels marked with an asterisk were considered known in the energy analysis.

[b]Errors are given in keV.

[c]Spin and parity assigned in Refs. 19 and 20.

Table II. Integrated cross sections of the ^{13}C levels observed in the ^{15}N(p,^{3}He)^{13}C reaction and comparison of these states with those previously reported.

^{15}N(p,^{3}He)^{13}C			Previously Reported[18]	
J^π	Excitation (MeV)	$\sigma_T(\mu b)$ (10-90°, c.m.)	J^π	Excitation (keV)
1/2⁻	*a 0.0 ± 15^b	308 ± 18	1/2⁻	0.0
1/2⁺	3.08 ± 20	very weak	1/2⁺	3.?86 ? 3
3/2⁻	*3.68 ± 10	573 ± 20	3/2⁻	3.6?1 ? 3
5/2⁺	*6.87 ± 15	42 ± 5	5/2⁺	6.866 ± 7
5/2⁻	7.55 ± 20	270 ± 18		7.55 ± 15
1/2⁻	8.86 ± 60	61 ± 9	1/2⁻	8.86 ± 20
(3/2⁻)	9.52 ± 30	71 ± 12		9.503 ± 15
(1/2⁻)	11.09 ± 50	52 ± 7		11.078 ± 20
(3/2⁻)	11.80 ± 30	137 ± 14		11.721 ± 30
7/2⁻	12.40 ± 50	100 ± 10	(1/2⁻)	12.45
3/2⁻	*15.11 ± 20	c88 ± 7	3/2⁻	15.113 ± 5
[T = 3/2]			[T = 3/2]	

a Levels marked with an asterisk were considered known in the energy analysis.

b Errors are given in keV.

c Integrated to 65°, c.m.

Table III. Optical model potentials.

$$-U(r) = Vf(r) + iWf(r) + 4aiW_D f'(r) - V_c(r)$$

Channel	V (MeV)	W (MeV)	W_D (MeV)	a_v (f)	a_w (f)	a_{w_D} (f)	r_v (f)	r_{w,w_D} (f)	r_c (f)
^{15}N+p (A)	34.0		22.0	0.65		0.50	1.25	1.25	1.30
^{13}N+t (X)	153.0		16.0	0.65		0.54	1.25	1.25	1.30
^{13}N+t (Y)	63.4	62.8		0.58	0.58		1.61	1.61	1.30
^{13}N+t (Z)	220.0	23.8		0.53	0.99		1.22	1.80	1.30

Table IV. Intermediate coupling predictions compared with experimental assignments for the mass 13 levels.

J^π	^{13}N (MeV)	^{13}C (MeV)	Kurath[33] a/k=5.5	Boyarkina[34] a/k=4.2	Barker[35] a/k=3.5	Halbert[36] et al.	Cohen and[5] Kurath
1/2⁻	0.0	0.0	0.0	0.0	0.0	0.0	0.0
3/2⁻	3.51	3.68	3.7	3.7	3.93	3.5	3.7
5/2⁻	7.38	7.55	5.3	6.1	7.11	7.0	7.4
1/2⁻	8.93	8.86	10.7	10.4	9.3	9.0	9.0
1/2⁻	10.78	11.09	12.5	12.4	11.3	-	13.8
3/2⁻	11.88	11.80	11.3	11.6	10.2	10.2	10.4
7/2⁻	-	12.40	12.0	12.3	13.5	-	11.1
3/2⁻ [T=3/2]	15.07	15.11	14.5	14.5	13.2	15.0	14.8
3/2⁻				15.2			14.0
5/2⁻				16.4			13.2
1/2⁻				22.2			17.4

Table V. Nuclear structure factors $(C_{ST}\ G_{NLSJT})^a$ for the states in mass 13.[b]

J^π	^{13}N (MeV)	^{13}C (MeV)	^{13}N NLSJT	$C_{ST}\ G_{NLSJT}$	^{13}C NLSJT	$C_{ST}\ G_{NLSJT}$
$1/2^-$	0.0	0.0	20001	.579	20110 20001 12110	.151 .284 -.462
$3/2^-$	3.51	3.68	12021	.565	20110 12021 12110 12120	.522 .278 .177 .380
$5/2^-$	7.38	7.55	12021	1.11	12120 12021 12130	-.562 .546 .151
$1/2^-$	8.93	8.86	20001	.0103	20110 20001 12110	.328 .00506 .172
$1/2^-$	10.78	11.09	20001	-.0972	20110 20001 12110	.0530 -.0481 -.185
$3/2^-$	11.88	11.80	12021	.256	20110 12021 12110 12120	.153 .127 .0921 -.471
$7/2^-$	-	12.40	-	-	12130	-.933
$3/2^-$	15.07	15.11	12021	.560	12021	.552

[T=3/2]

[a] See Ref. 4 for a definition of $C_{ST}\ G_{NLSJT}$. The values shown in the table do not include the L=0 N=1 terms since these make little contribution to the cross section.

[b] We are indebted to Dr. Kurath for providing us with the appropriate two-nucleon coefficients of fractional parentage.

Table VI. $^{15}N(p,t)^{13}N$ relative cross sections for different form factors and optical model potentials.

J^π	Exc. (MeV)	$\sigma_T(\mu b)$ exp. (10-90°, c.m.)	Relative σ_T (exp.)	Matching R(f)	AX σ_T (Rel.)	AZ σ_T (Rel.)	ν	AX σ_T (Rel.)	AZ σ_T (Rel.)
1/2⁻	0.0	941	1.00	3.58	.200[a]	.500	.318	.400[a]	.790
3/2⁻	3.51	652	.693	3.70	.444	.510	.334	.676	.616
5/2⁻	7.38	1271	1.35	3.82	2.06	1.92	.348	2.22	1.73
1/2⁻	8.93	130	.138	[3.84	.00024	.00025][b]	[.351	.00021	.00022][b]
1/2⁻	10.78	17.6	.0187	3.89	.0266	.0244	.357	.0184	.0188
							[.357	.0968	.0675][b]
3/2⁻	11.88	93	.0988	3.94	.120	.0900	.362	.0855	.0576
3/2⁻	15.07	115	.122	4.03	.544	.359	.372	.263	.181
[T=3/2]									
					B = 1.53	0.68		0.59	0.31

[a] The ground state is expected to show poor agreement for the AX potential since this potential produced a relatively poor fit to the data (Fig. 15).

[b] Not included in the calculation of B.

Table VII. $^{15}N(p,^3He)^{13}C$ relative cross sections for different spin-dependent interactions and optical model potentials.

J^π	Exc. (MeV)	σ_T(μb) exp. (10-90°,c.m.)	Relative σ_T (exp.)	$A^S = A^T$ AX σ_T (Rel.)	AZ σ_T (Rel.)	$A^S = 0.3 A^T$ AX σ_T (Rel.)	AZ σ_T (Rel.)	ν
1/2⁻	0.0	308	1.00	.650	1.00	.612	.997	.308
3/2⁻	3.68	573	1.86	1.04	1.44	1.04	1.28	.323
5/2⁻	7.55	270	.878	1.41	1.26	2.00	1.66	.337
1/2⁻	8.86	61	.198	.271	.329	.198	.226	.342
(1/2⁻)	11.09	52	.169	.0690	.0588	.0571	.0479	.350
(3/2⁻)	11.80	137	.445	.444	.364	.361	.276	.352
7/2⁻	12.40	100	.325	1.31	1.02	.954	.693	.354
3/2⁻ [T=3/2]	15.11	115ᵃ	.358	.319	.246	.699	.395	.363
			B_1 =	0.863	0.760	0.972	0.733	
			B_2^b =	0.498	0.426	0.899	0.710	

ᵃThis cross section assumed identical to the (p,t) [T=3/2] cross section due to the lack of large angle data.

ᵇThis calculation does not include the 8.86 MeV (1/2⁻) and 12.40 MeV (7/2⁻) levels.

REFERENCES

1. J. Cerny and R. H. Pehl, Phys. Rev. Letters 12, 619 (1964); J. Cerny,
    R. H. Pehl and G. T. Garvey, Phys. Letters 12, 234 (1964); G. T. Garvey,
    J. Cerny and R. H. Pehl, Phys. Rev. Letters 12, 726 (1964); C. Detraz,
    J. Cerny and R. H. Pehl, Phys. Rev. Letters 14, 708 (1965); J. Cerny,
    R. H. Pehl, G. Butler, D. G. Fleming, C. Maples and C. Detraz, Phys.
    Letters 20, 35 (1966).

2. J. Cerny, C. Detraz and R. H. Pehl, Phys. Rev. 152, 950 (1966).

3. N. K. Glendenning, Ann. Rev. Nucl. Sci. 13, 191 (1963).

4. N. K. Glendenning, Phys. Rev. 137B, 102 (1965).

5. S. Cohen and D. Kurath, Nucl. Phys. 73, 1 (1965), and D. Kurath, private
    communication.

6. J. J. Wesolowski, L. F. Hansen, J. G. Vidal and M. L. Stelts, Phys. Rev.
    148, 1063 (1966); J. Vervier, Phys. Letters 22, 82 (1966) and 24B, 603
    (1967); R. K. Cole, R. Dittman, H. S. Sandhu and C. N. Waddell, Nucl.
    Phys. A91, 665 (1967).

7. R. A. Broglia and C. Riedel, Nucl. Phys. A92, 145 (1967) and A93, 241 (1967).

8. N. F. Mangelson and B. G. Harvey, Lawrence Radiation Laboratory Annual
    Report, UCRL-17299, p. 97, 1966 (unpublished) and N. F. Mangelson, pri-
    vate communication.

9. N. K. Glendenning, Phys. Rev. 156, 1344 (1967).

10. C. L. Lin and S. Yoshida, Prog. Theo. Phys. (Tokyo) 32, 885 (1964);
    E. M. Henley and D. V. L. Yu, Phys. Rev. 133B, 1445 (1964); B. Bayman,
    Argonne National Laboratory Report, ANL-6878, p. 335, 1964 (unpublished);
    A.Y. Abul-Magd and M. El. Nadi, Nucl. Phys. 77, 182 (1966); C. Lin, Prog.
    Theo. Phys. (Tokyo) 36, 251 (1966).

11. J. R. Rook and D. Mitra, Nucl. Phys. $\underline{51}$, 96 (1964); J. R. Rook and V. S. Mathur, Nucl. Phys. $\underline{A91}$, 305 (1967).

12. We assume pure relative-s state motions, which is known to be at least 94% good for the triton g.s. [J. M. Blatt, G. H. Derrick and J. N. Lyness, Phys. Rev. Letters $\underline{8}$, 323 (1962); R. Pascual, Phys. Letters $\underline{19}$, 221 (1965); B. F. Gibson, Phys. Rev. $\underline{139}$, 1153 (1965)].

13. These parentage factors (with the possible exception of a phase change) are generally true for any two-nucleon transfer reaction on an odd mass target which involves a single (extra-core) nucleon.

14. C. Schwartz and A. de-Shalit, Phys. Rev. $\underline{94}$, 1257 (1954).

15. D. G. Fleming, Ph.D. Thesis, University of California Lawrence Radiation Laboratory Report, UCRL-17790, 1967.

16. Hamilton Watch Co., Lancaster, Pa.

17. F. S. Goulding, D. A. Landis, J. Cerny and R. H. Pehl, Nucl. Instr. and Methods $\underline{31}$, 1 (1964).

18. F. A. Selove, Energy Levels of Light Nuclei, May 1962, NAS-NRC, and private communication.

19. G. Ball and J. Cerny, to be published.

20. D. Bachelier, M. Bernas, I. Brissaud, P. Radvanyi and M. Roy, Nucl. Phys. $\underline{88}$, 307 (1966); R. L. Kozub, L. A. Kull and E. Kashy, Nucl. Phys. $\underline{A99}$ 540 (1967).

21. G. Bassani, N. M. Hintz, C. D. Kavaloski, J. R. Maxwell and G. M. Reynolds, Phys. Rev. $\underline{139B}$, 830 (1965); J. R. Maxwell, G. M. Reynolds and N. M. Hintz, Phys. Rev. $\underline{151}$, 1000 (1966); J. R. Maxwell, G. M. Reynolds and N. M. Hintz, Phys. Letters $\underline{22}$, 454 (1966); G. M. Reynolds, J. R. Maxwell and N. M. Hintz, Phys. Rev. $\underline{153}$, 1283 (1967).

22. M. P. Fricke and G. R. Satchler, Phys. Rev. 139B, 567 (1965); E. T. Boschitz, M. Chabre, H. E. Conzett and R. J. Slobodrian, Lawrence Radiation Laboratory Annual Report, UCRL-16580, 1965, p. 118 (unpublished); J. A. Fannan, E. J. Burge, D. A. Smith and N. K. Ganguly, Nucl. Phys. A97, 263 (1967).

23. A. E. Glassgold and P. J. Kellog, Phys. Rev. 109, 1291 (1958).

24. F. Bjorklund, Proceedings of the International Conference on Nuclear Optical Model, Florida State University, 1959; p. 1.

25. R. N. Glover and A. D. W. Jones, Phys. Letters 16, 69 (1965); J. R. Rook, Nucl. Phys. 61, 219 (1965); K. R. Greider and W. R. Dodd, Phys. Rev. 146, 671 (1966).

26. R. N. Glover and A. D. W. Jones, Nucl. Phys. 81, 277 (1966).

27. W. W. Daehnick, Phys. Rev. 135B, 1168 (1964); B. Johansson, Nucl. Phys. 67, 285 (1965); J. Stevens, H. F. Lutz and S. F. Eccles, Nucl. Phys. 76, 129 (1966); A. J. Frasca, R. W. Finlay, R. O. Koshel and R. L. Cassola, Phys. Rev. 144, 854 (1966).

28. J. C. Hiebert, E. Newman and R. H. Bassel, Phys. Rev. 154, 898 (1967).

29. P. E. Hodgson, Proceedings of the Rutherford Julilee International Conference, Manchester, England, 1961, edited by J. B. Birks (Heywood and Company, Ltd., London, 1962) p. 407; H. M. Sen Gupta, J. Rotblatt, P. E. Hodgson and J. B. A. England, Nucl. Phys. 38, 361 (1962).

30. F. G. Perey, Phys. Rev. 131, 745 (1963); P. C. Sood, Nucl. Phys. 84, 106 (1966).

31. D. R. Inglis, Rev. Mod. Phys. 25, 390 (1953).

32. A. M. Lane, Proc. Phys. Soc. (London) A66, 977 (1953) and A68, 197 (1954).

33. D. Kurath, Phys. Rev. 101, 216 (1956).

34. A. N. Boyarkina, Akademia Nauk, USSR (English translation), Physical Series 28, 255 (1964).

35. F. C. Barker, Nucl. Phys. 45, 467 (1963).

36. E. C. Halbert, Y. E. Kim and T. T. S. Kuo, Phys. Letters $\underline{20}$, 657 (1966).

37. T. Hamada and I. D. Johnston, Nucl. Phys. $\underline{34}$, 383 (1962).

38. F. C. Barker, Nucl. Phys. $\underline{83}$, 418 (1966).

39. W. M. True, Phys. Rev. $\underline{130}$, 1530 (1963).

40. Both of these levels could not be resolved from neighboring $5/2^+$ states at 3.56 MeV in ^{13}N and 3.85 MeV in ^{13}C. However, as is later discussed, a $5/2^+$ transition cannot be directly excited by two-nucleon transfer in the 1p shell, so that any contribution of these $(5/2^+)$ levels to the cross sections of the allowed $(3/2^-)$ states is thought to be small.

41. G. G. Shute, D. Robson, V. R. McKenna and A. T. Berztiss, Nucl. Phys. $\underline{37}$, 535 (1962).

42. H. S. Adams, J. D. Fox, N. P. Heydenburg and G. M. Temmer, Phys. Rev. $\underline{124}$, 1899 (1961); M. Nomoto, Nucl. Phys. $\underline{30}$, 514 (1962).

43. F. C. Barker, Nucl. Phys. $\underline{45}$, 449 (1963).

44. A. Gallman, D. E. Alburger, D. H. Wilkinson and F. Hibou, Phys. Rev. $\underline{129}$, 1965 (1963).

45. G. G. Shute and A. M. Baxter, Nucl. Phys. $\underline{83}$, 460 (1966).

46. R. McPherson, R. A. Esterlund, A. M. Poskanzer, and P. L. Reeder, Phys. Rev. $\underline{140B}$, 1513 (1965).

47. A. Marques, A. J. P. L. Policarpo and W. R. Phillips, Nucl. Phys. $\underline{36}$, 45 (1962).

48. D. E. Grace and B. D. Sowerby, Nature $\underline{206}$, 494 (1965).

49. T. W. Bonner, A. A. Kraus, Jr., J. B. Marion and J. P. Schiffer, Phys. Rev. $\underline{102}$, 1348 (1956); J. H. Gibbons and R. H. Macklin, Phys. Rev. $\underline{137B}$. 1508 (1965).

50. There is a known[18] $7/2^-$ state at lower excitation -10.36 MeV in ^{13}N - which is excited by an f wave resonance in ^{12}C+p scattering.[41] As such, it does not appear in an intermediate coupling calculation restricted to the 1p shell. This 10.36 MeV ($7/2^-$) level is very weakly excited in the ^{15}N(p,t)^{13}N reaction and there is no evidence for a level at this excitation in the (p,^{3}He) spectrum.

51. J. Cerny, R. H. Pehl, G. Butler, D. G. Fleming, C. Maples and C. Detraz, Phys. Letters 20, 35 (1966).

52. D. G. Fleming, J. Cerny and N. K. Glendenning, submitted to the Physical Review.

53. G. Strobel, Phys. Rev. 154, 941 (1967).

54. J. Cerny, D. G. Fleming and C. C. Maples, unpublished data; J. R. Maxwell, G. M. Reynolds and N. M. Hintz, University of Minnesota Annual Progress Report, 1965, p. 98. (unpublished).

55. N. Austern, Phys. Rev. 136B, 1743 (1964); R. Sherr, B. F. Bayman, E. Rost, M. E. Rickey and C. G. Hoot, Phys. Rev. 139B, 1272 (1965); C. Glashausser, M. Kondo, M. E. Rickey and E. Rost, Phys. Letters 14, 113 (1965).

56. F. C. Barker, Nucl. Phys. 28, 96 (1961); T. Sebe, Prog. Theor. Phys. (Tokyo) 30, 290 (1963).

57. G. C. Ball and J. Cerny, Phys. Letters 21, 551 (1966). and G. C. Ball, private communication.

58. S. K. Penny and G. R. Satchler, Nucl. Phys. 53, 145 (1964); B. Kozlowsky and A. de-Shalit, Nucl. Phys. 77, 215 (1966); S. K. Penny, Ph.D. Thesis, University of Tennessee, 1966 (unpublished); F. S. Levin, Phys. Rev. 147, 715 (1966).

UCRL-17840

59. J. C. Hardy and I. S. Towner, Phys. Letters 25B, 98 (1967).

60. R. E. Brown, N. M. Hintz, C. G. Hoot, J. R. Maxwell and A. Scott,

     University of Minnesota Annual Progress Report, 1966, p. 70 (unpublished).

FIGURE CAPTIONS

Fig. 1. Cyclotron layout and beam optics.

Fig. 2. A counter assembly and block diagram of the electronics used in these experiments.

Fig. 3. A typical particle - identifier spectrum.

Fig. 4. Energy spectra for the $^{15}N(p,t)^{13}N$ and $^{15}N(p,^{3}He)^{13}C$ reactions. The spectra have been adjusted to match channels for the $5/2^{-}$ transitions, showing a slight non-linearity in the triton spectrum at the higher energies.

Fig. 5. Energy level diagram for ^{13}N and ^{13}C.

Fig. 6. Energy spectra of the $^{14}N(d,^{3}He)^{13}C$ and $^{14}N(^{3}He,\alpha)^{13}N$ reactions.

Fig. 7. $^{15}N(p,t)^{13}N$ L=0 angular distributions. The curves are drawn through the data and have no theoretical significance.

Fig. 8. $^{15}N(p,t)^{13}N$ L=2 angular distributions. The curves have no theoretical significance.

Fig. 9. Angular distributions for the $^{13}C(p,t)^{11}C$ 6.49 MeV, the $^{15}N(p,t)^{13}N$ 6.38 MeV and the $^{15}N(p,^{3}He)^{13}C$ 6.87 MeV transitions. The curves have no theoretical significance.

Fig. 10. The L=0,2 angular distributions of the $^{15}N(p,^{3}He)^{13}C$ g.s. and 3.68 MeV transitions. The curves have no theoretical significance.

Fig. 11. $^{15}N(p,^{3}He)^{13}C$ L=0, L=2 angular distributions. The curves have no theoretical significance.

Fig. 12. $^{15}N(p,^{3}He)^{13}C$ L=2 angular distributions. The curves have no theoretical significance.

Fig. 13. "Standard" (p,t) L=0 angular distributions obtained on a variety of light nuclei.

Fig. 14. "Standard"(p,t) L=2 angular distributions obtained on a variety of light nuclei.

Fig. 15. DWBA fits to the $^{15}N(p,t)^{13}N$ g.s. (1/2$^-$, L=0) transition, utilizing the AX, AY and AZ optical model potentials given in Table III.

Fig. 16. DWBA fits to the $^{15}N(p,t)^{13}N$ 7.38 MeV (5/2$^-$, L=2) transition, utilizing the AX, AY and AZ optical model potentials given in Table III.

Fig. 17. DWBA fits to the $^{15}N(p,t)^{13}N$ g.s. and $^{15}N(p,^3He)^{13}C$ g.s. transitions.

Fig. 18. DWBA fits to the $^{15}N(p,t)^{13}N$ 3.51 MeV and $^{15}N(p,^3He)^{13}C$ 3.68 MeV transitions.

Fig. 19. DWBA fits to the $^{15}N(p,t)^{13}N$ 7.38 MeV and $^{15}N(p,^3He)^{13}C$ 7.55 MeV transitions.

Fig. 20. DWBA fits to the $^{15}N(p,t)^{13}N$ 8.93 MeV and $^{15}N(p,^3He)^{13}C$ 8.86 MeV transitions.

Fig. 21. DWBA fits to the $^{15}N(p,t)^{13}N$ 10.78 MeV and $^{15}N(p,^3He)^{13}C$ 11.09 MeV transitions.

Fig. 22. DWBA fits to the $^{15}N(p,t)^{13}N$ 11.88 MeV (L=2) and $^{15}N(p,^3He)^{13}C$ 11.80 MeV transitions. A representative L=0 fit is also shown for the (p,t) reaction.

Fig. 23. DWBA fits to the $^{15}N(p,^3He)^{13}C$ 12.40 MeV and $^{15}N(p,t)^{13}N$ 15.07 MeV (T=3/2) transitions.

Fig. 24. DWBA fits to the $^{13}C(p,t)^{11}C$ 6.49 MeV and $^{15}N(p,t)^{13}N$ 6.38 MeV transitions, utilizing different choices for the oscillator parameter ν in the bound state wave function.

Fig. 1

MUB-11780

Scale

0   5   10
feet

0   1   2   3   4   5
meters

Box
4-in. gate valve
Collimator
Guillotine
Quadrupole lens doublet
Detector holder and
collimating system

Faraday cup

Foil wheel

System 2

Magnet

Target holder
(vertical and radial focus)

System 1

Final
collimator

Beam viewing and
alignment box

Quad 22

20-inch
scatter chamber

Quad 21

Concrete shielding

Steel shielding

Analyzing slit
(2nd radial focus)

Beam plug

1st vertical
focus

Beam analysis
magnet

Radial
collimator

Virtual
source

Beam
deflector

Quartz viewing plate
(1st radial focus)

Quad 3

Beam

Quad 1

Pole face edge

Vertical
collimator

Cyclotron
vacuum tank

XBL 678-4476

Fig. 2

Fig. 3

MUB-4293

$^{15}N(p, ^3He)^{13}C$
15 deg

15.11 MeV
3/2⁻, T=3/2

12.40 MeV
7/2⁻

11.80 MeV
(3/2⁻)

9.52 MeV
(3/2⁻)

11.09
MeV
(1/2⁻)

8.86 MeV
1/2⁻

3.68 MeV
3/2⁻

g.s.
1/2⁻

7.55 MeV
5/2⁻

6.87 MeV
5/2⁺

3.08 MeV
1/2⁺

× 1/8

$^{15}N(p, t)^{13}N$
15 deg

15.07 MeV
3/2⁻, T=3/2

11.88 MeV
3/2⁻

10.78 MeV
1/2⁻

8.93 MeV
1/2⁻

7.38 MeV
5/2⁻

605

3.51 MeV
3/2⁻

559

g.s.
1/2⁻

6.38 MeV
5/2⁺

2.36 MeV
1/2⁺

× 1/4

Counts per channel

Channel number

XBL677-3550

Fig. 4

XBL677-3549

Fig. 5
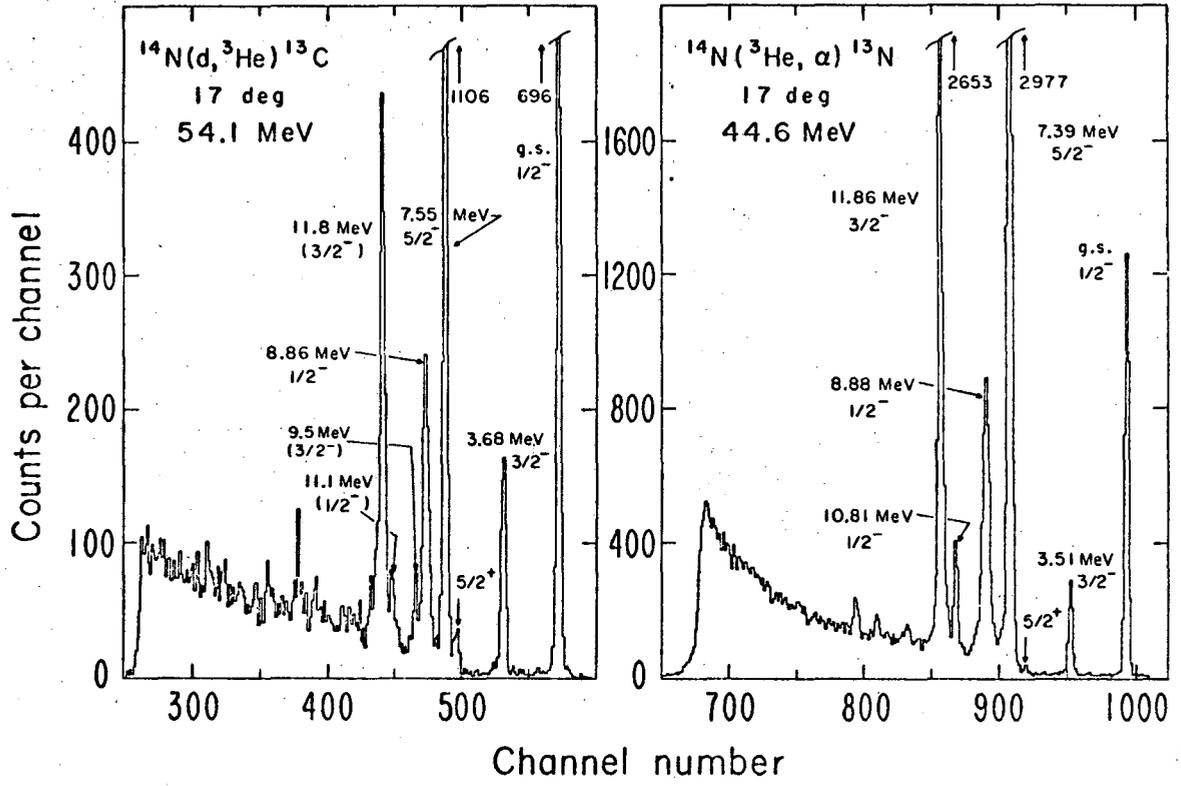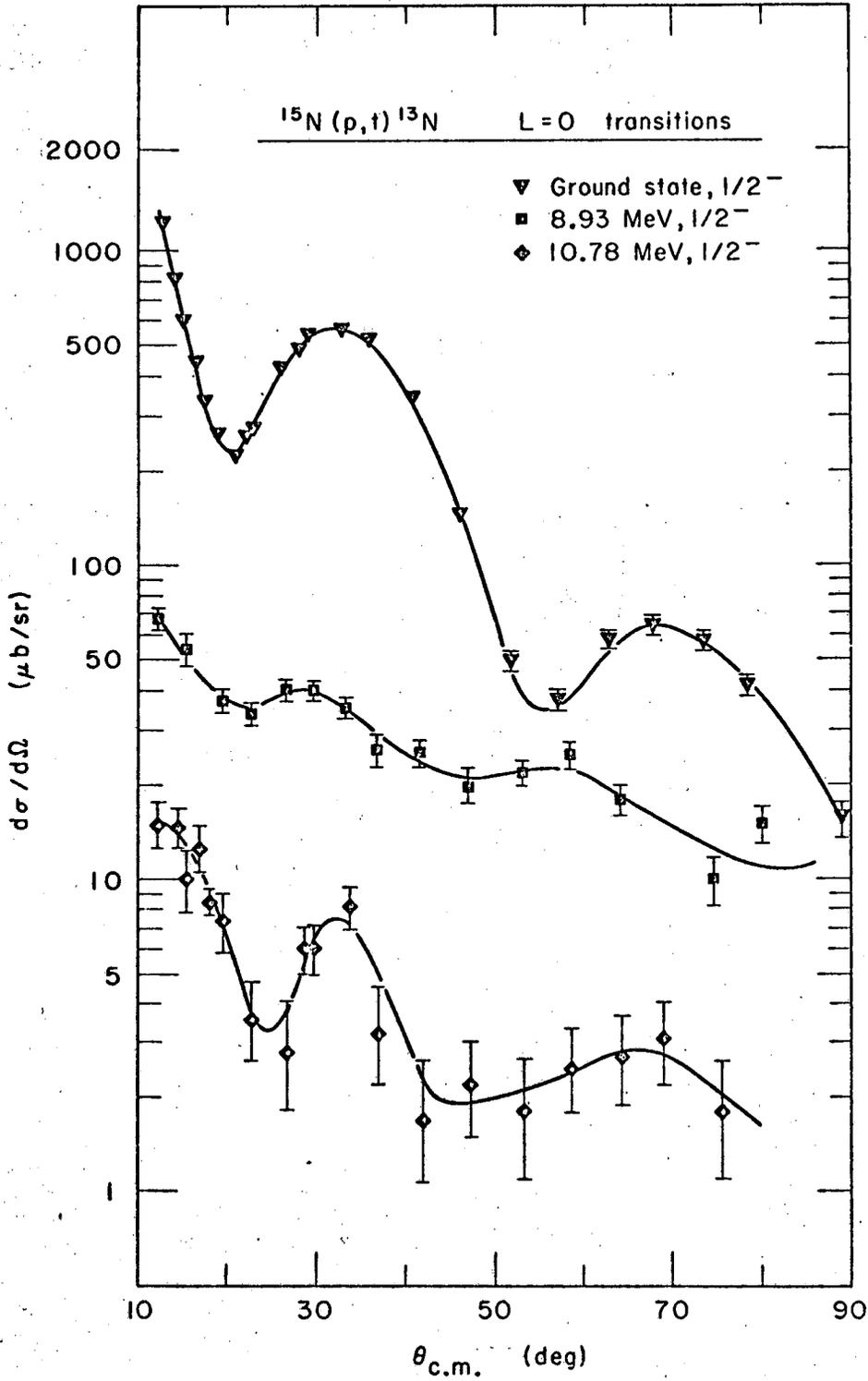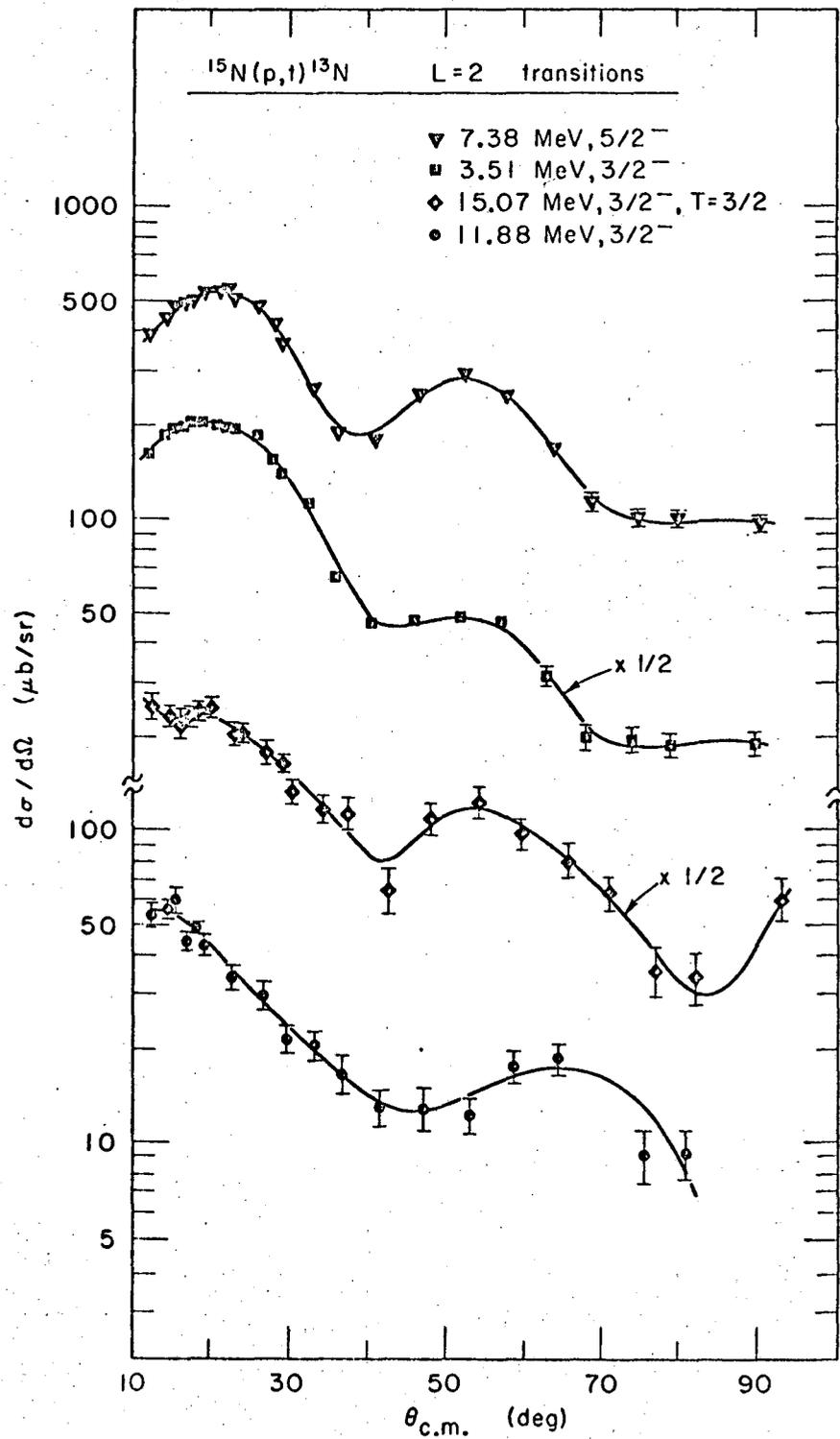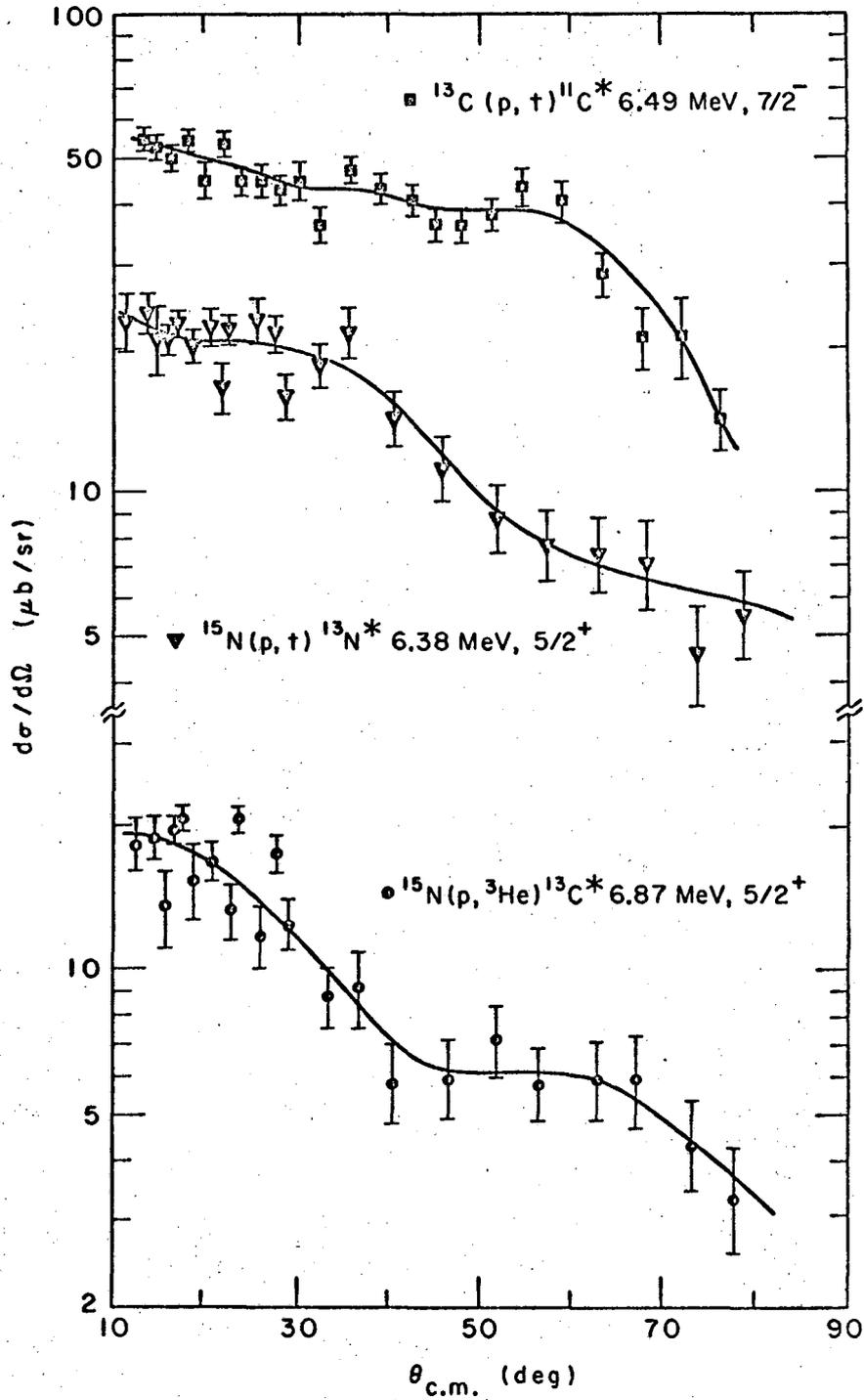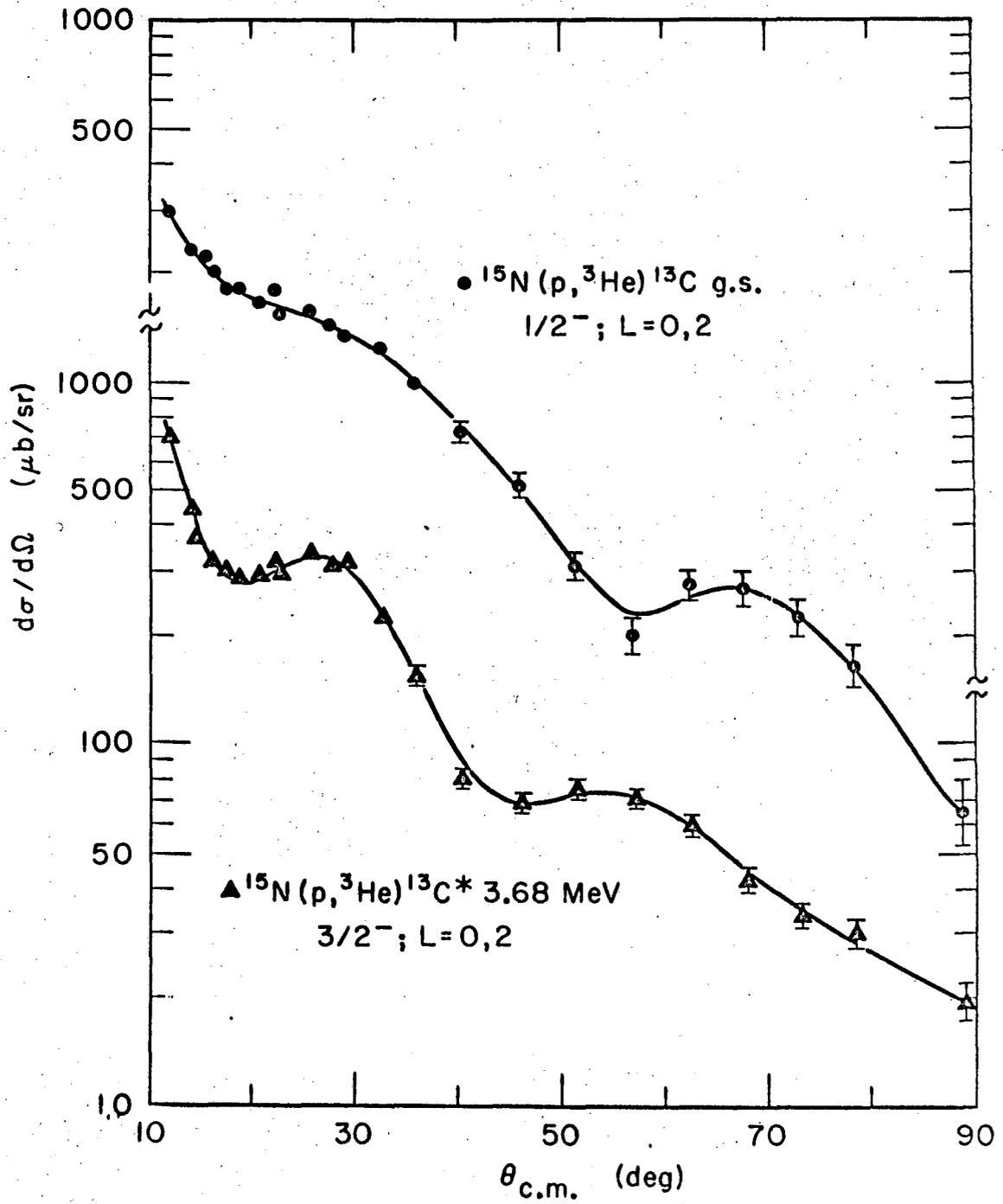
Fig. 6

XBL677-3548

$^{15}N(p,t)^{13}N$ L = 0   transitions

▽ Ground state, 1/2⁻
▣ 8.93 MeV, 1/2⁻
◈ 10.78 MeV, 1/2⁻

$d\sigma/d\Omega$ $(\mu b/sr)$

$\theta_{c.m.}$ (deg)

XBL676-3271-A

Fig. 7

$^{15}N(p,t)^{13}N$ L=2   transitions

▽ 7.38 MeV, 5/2⁻
▯ 3.51 MeV, 3/2⁻
◇ 15.07 MeV, 3/2⁻, T=3/2
● 11.88 MeV, 3/2⁻
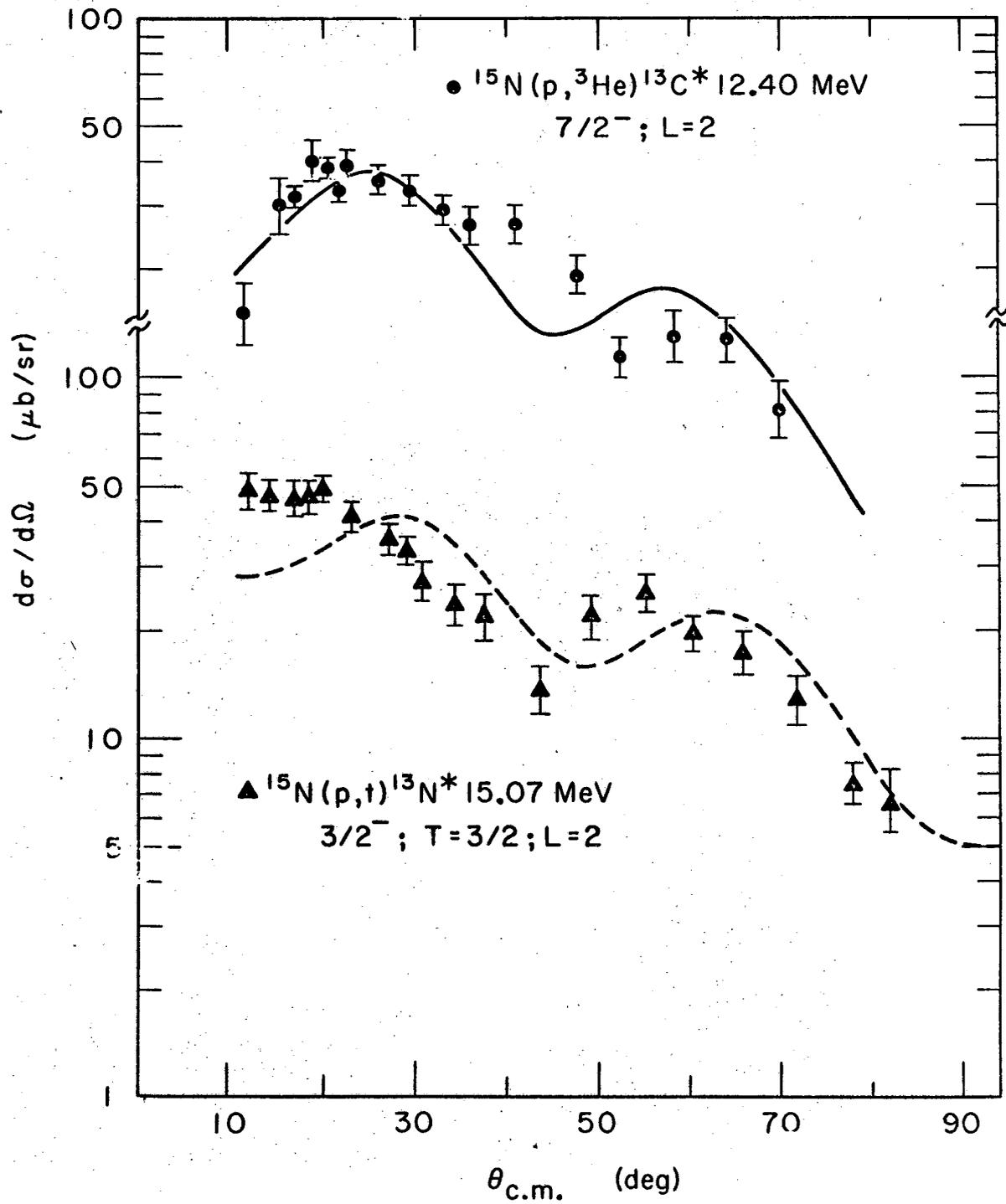
XBL676-3269-A

Fig. 8

XBL678-3730

Fig. 9

XBL676-3268-A

Fig. 10

^{15}N (p,^{3}He)^{13}C   L = 0,2   transitions

▲ 8.86 MeV, 1/2$^-$
■ 9.52 MeV (3/2$^-$)
▼ 11.09 MeV (1/2$^-$)
● 11.80 MeV (3/2$^-$)

XBL 676 - 3266-A

Fig. 11

$^{15}N(p,^3He)^{13}C$ L=2 transitions

▲ 7.55 MeV, 5/2⁻
● 12.40 MeV, 7/2⁻
▼ 15.11 MeV, 3/2⁻, T=3/2

XBL676-3270-A

Fig.12

Fig. 13

MUB-11572

Fig. 14

MUB·11571

XBL 676-3273

Fig. 15

$^{15}N(p,t)^{13}N^*$ 7.38 MeV
$5/2^-$; L=2

Pot. AX
Pot. AY
Pot. AZ

$d\sigma/d\Omega$ (μb/sr)

$\theta_{c.m.}$ (deg)
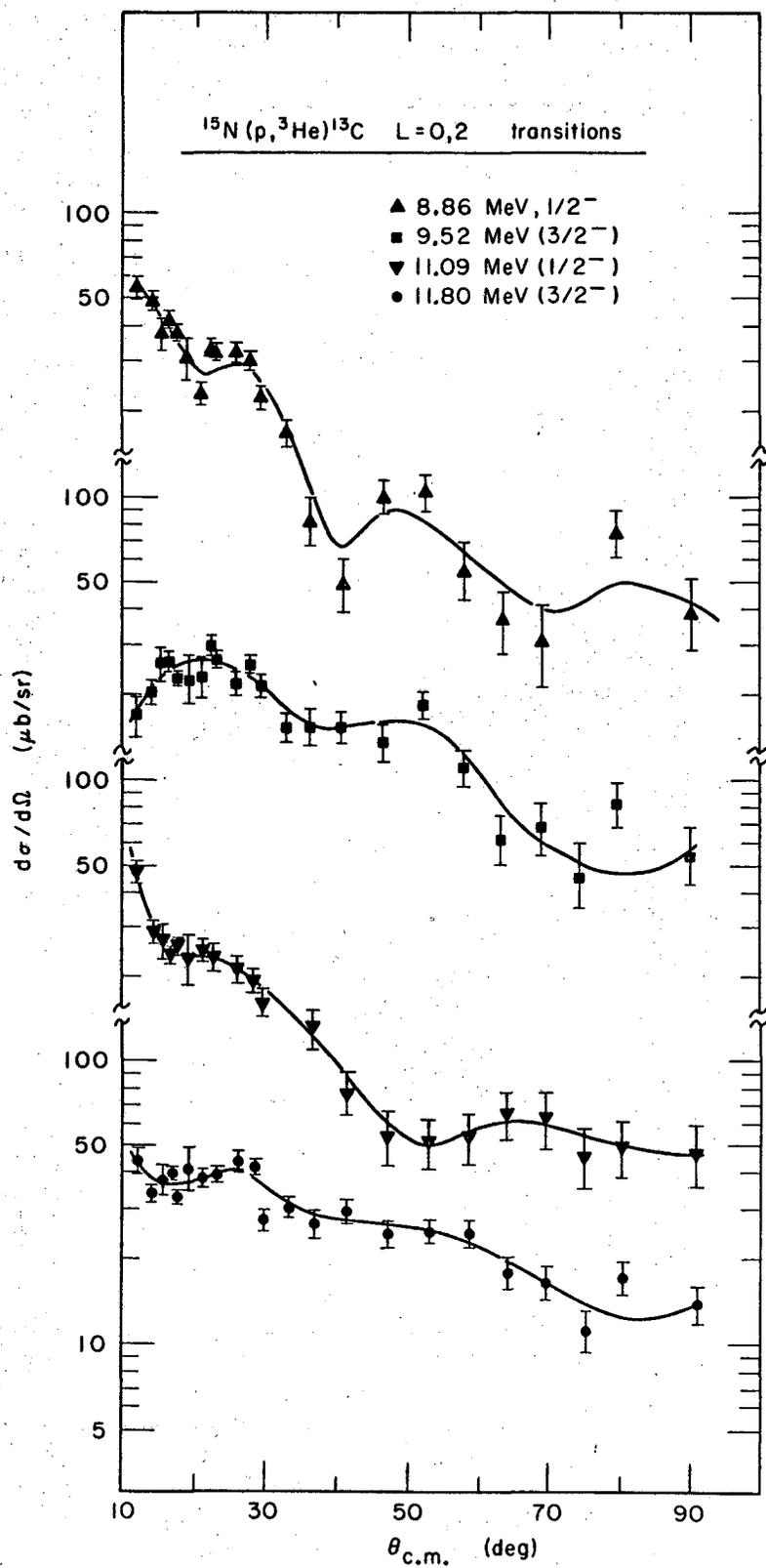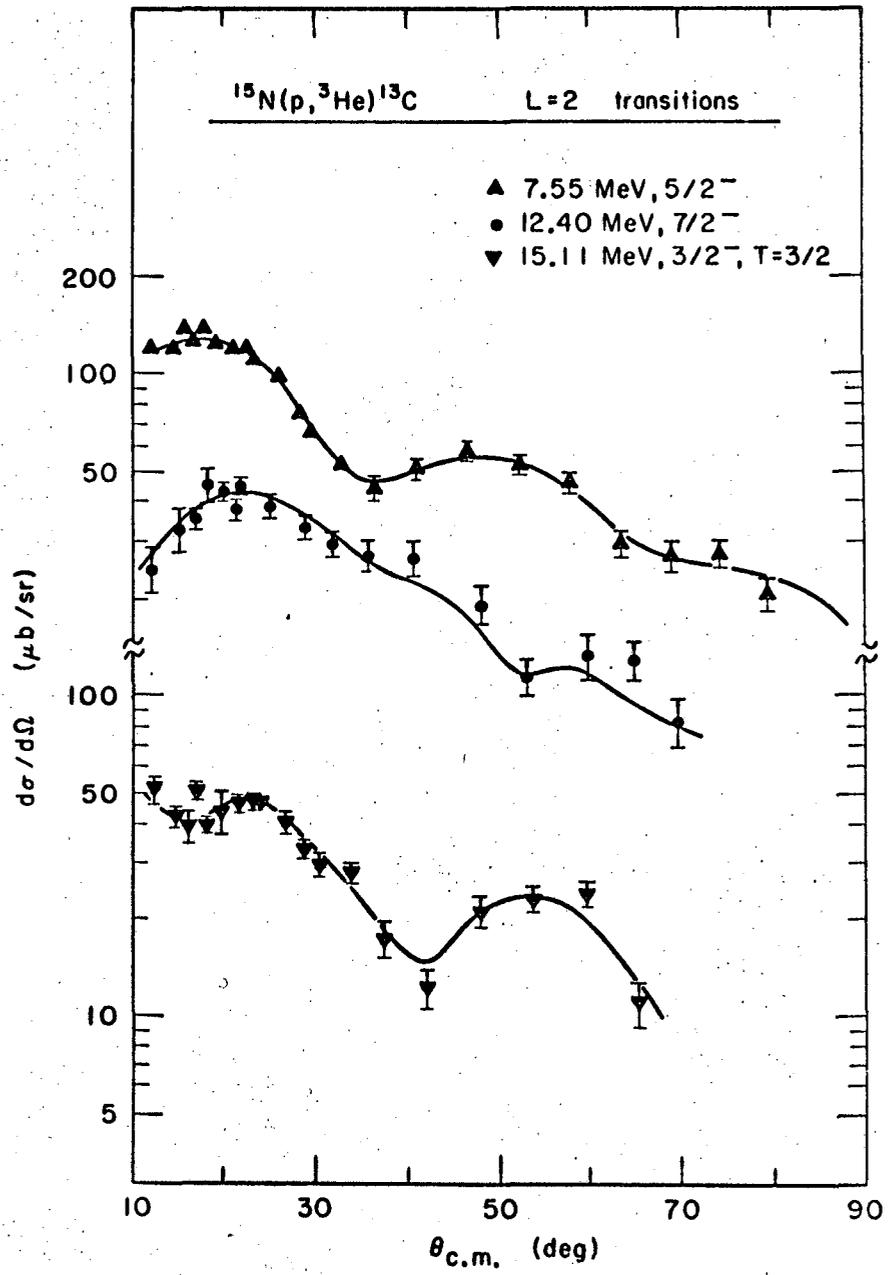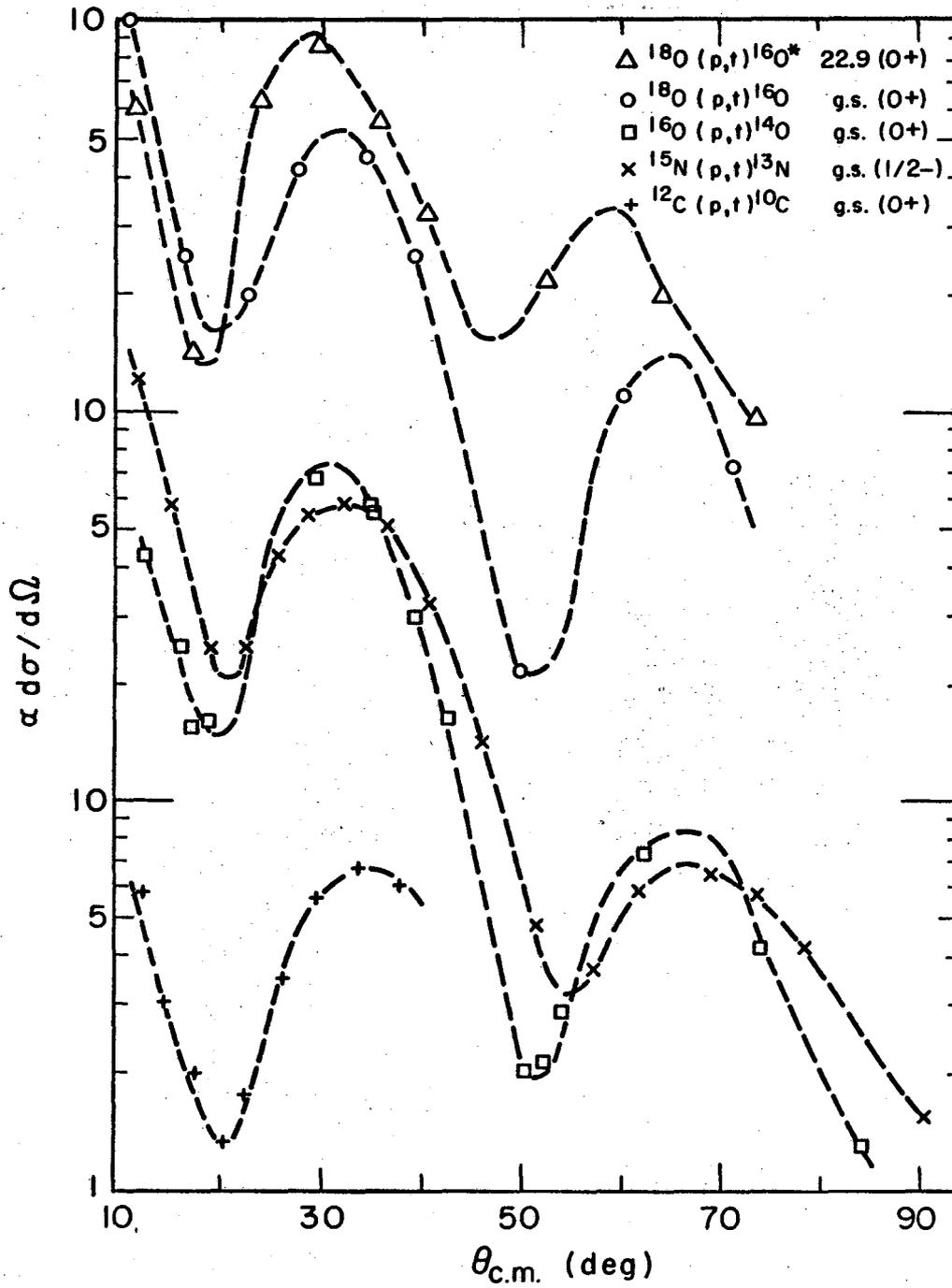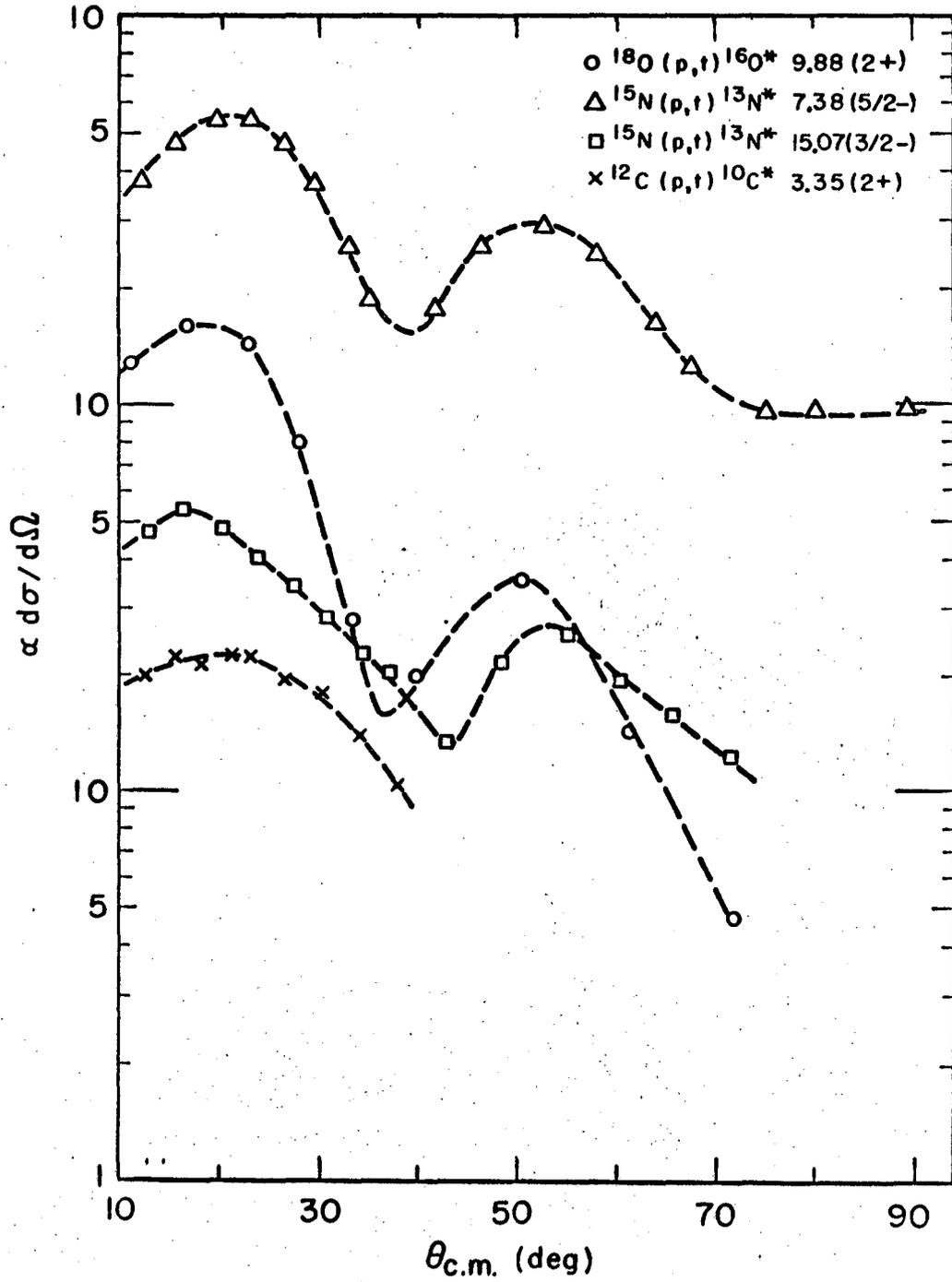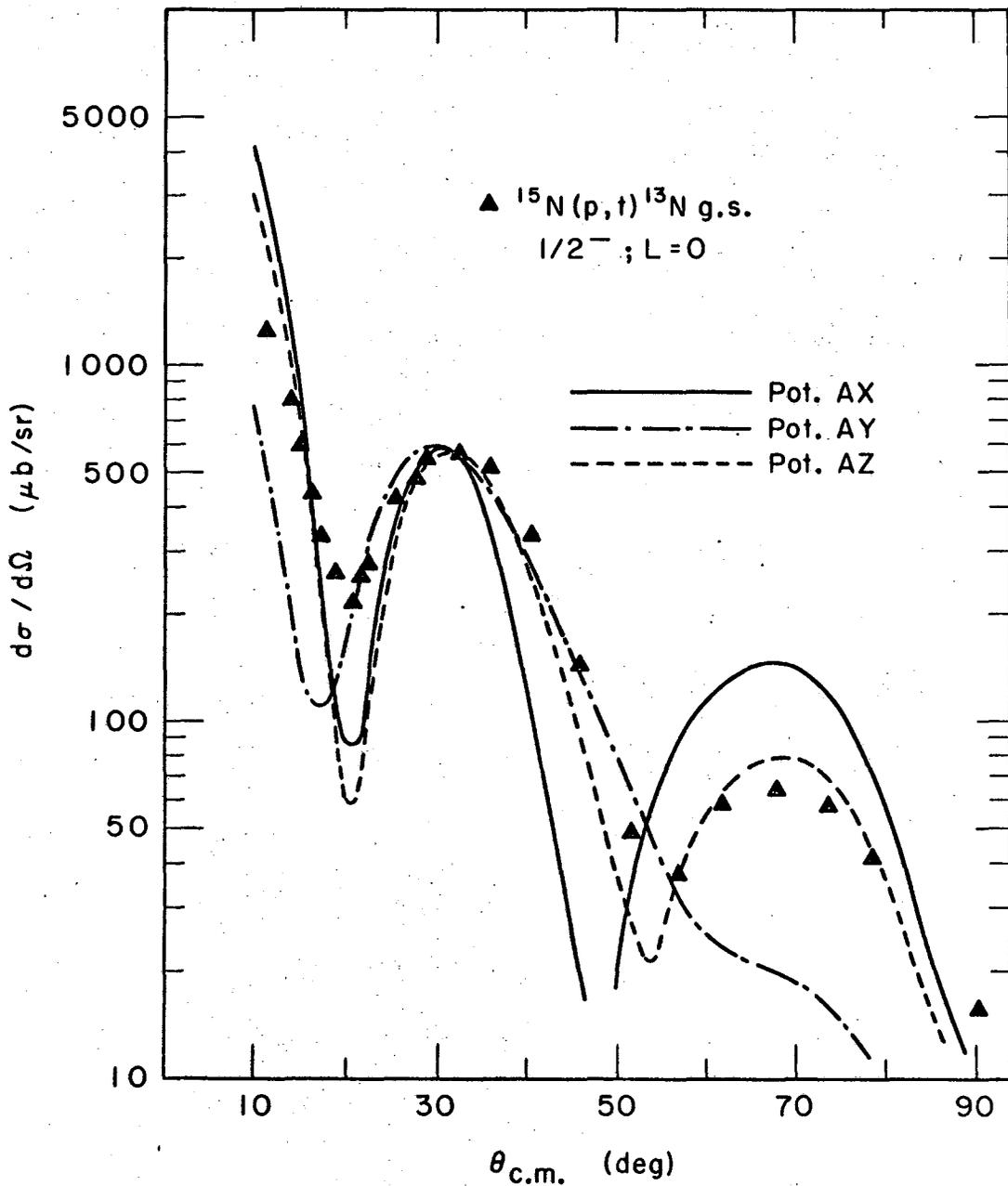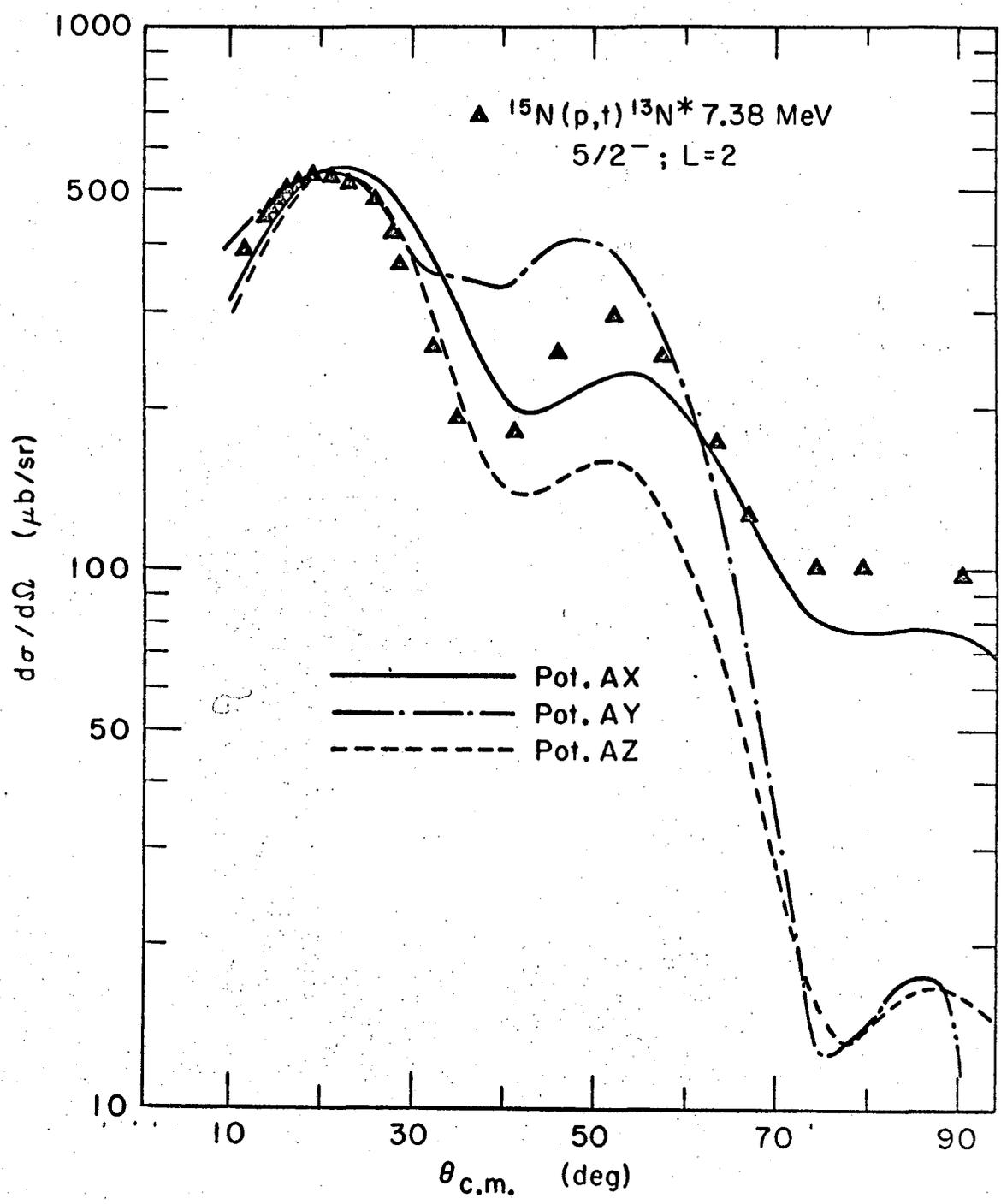
XBL676-3277-A

Fig. 16
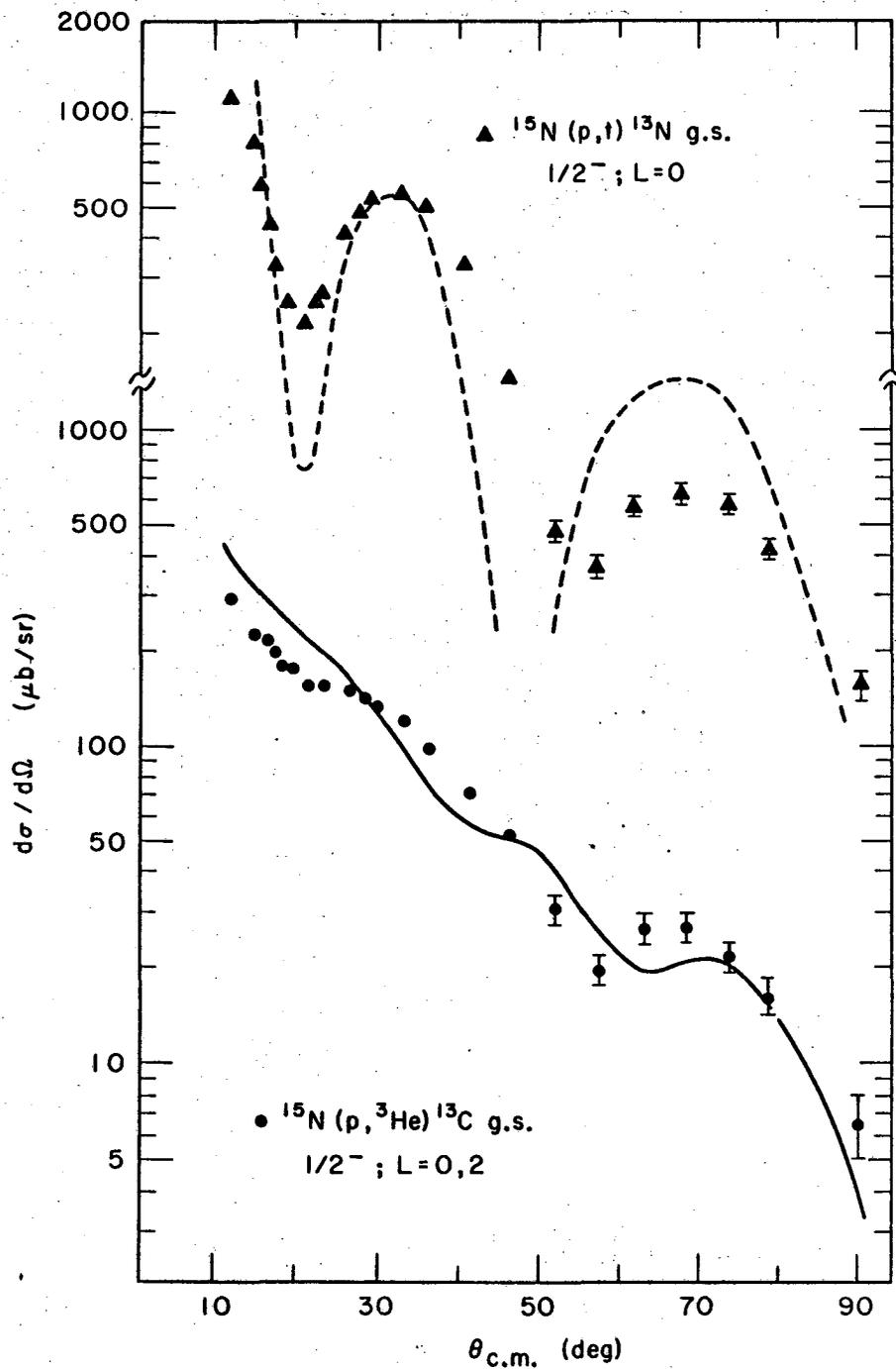
XBL676-3272

Fig. 17
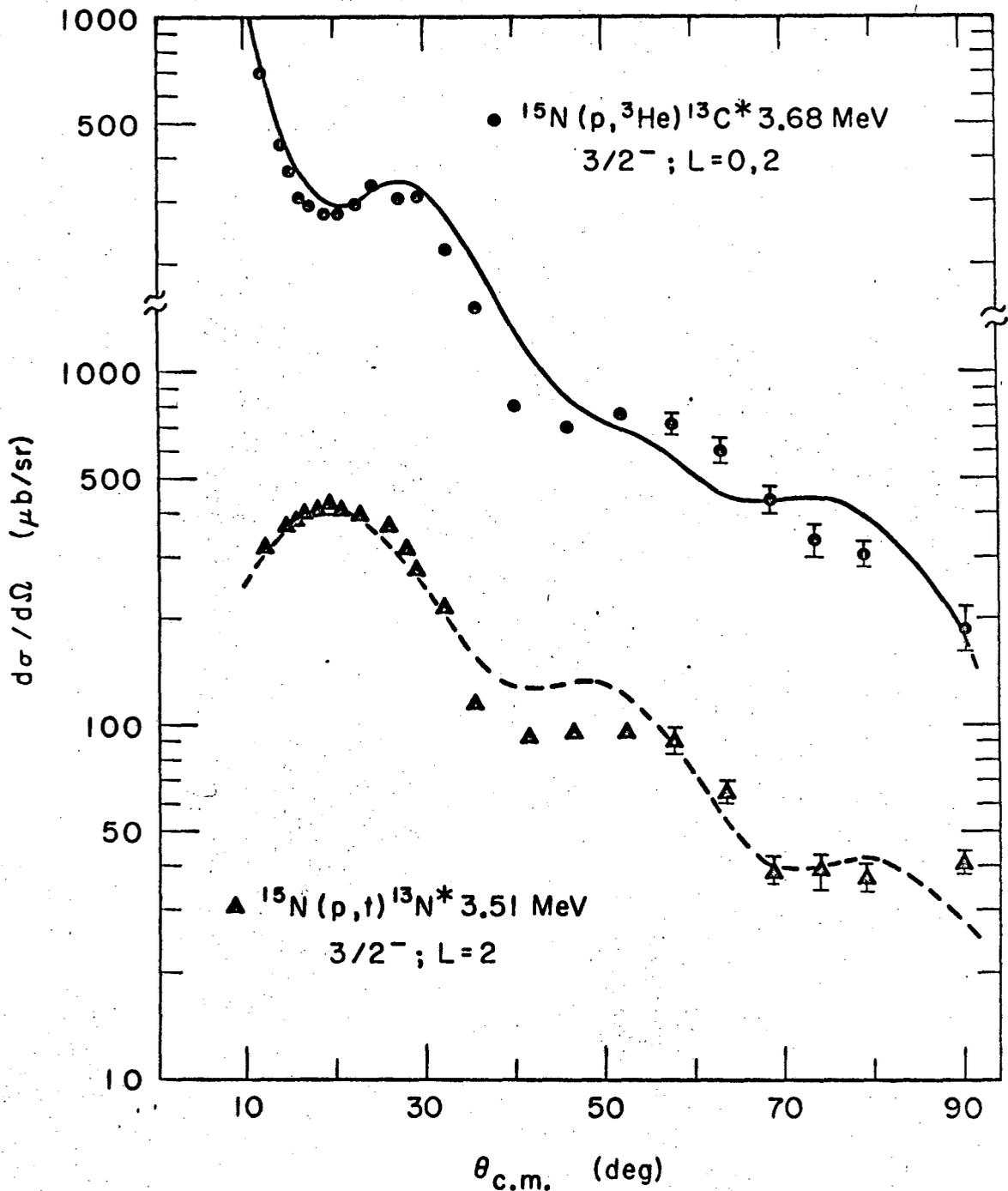
XBL676-3279-A

Fig. 18
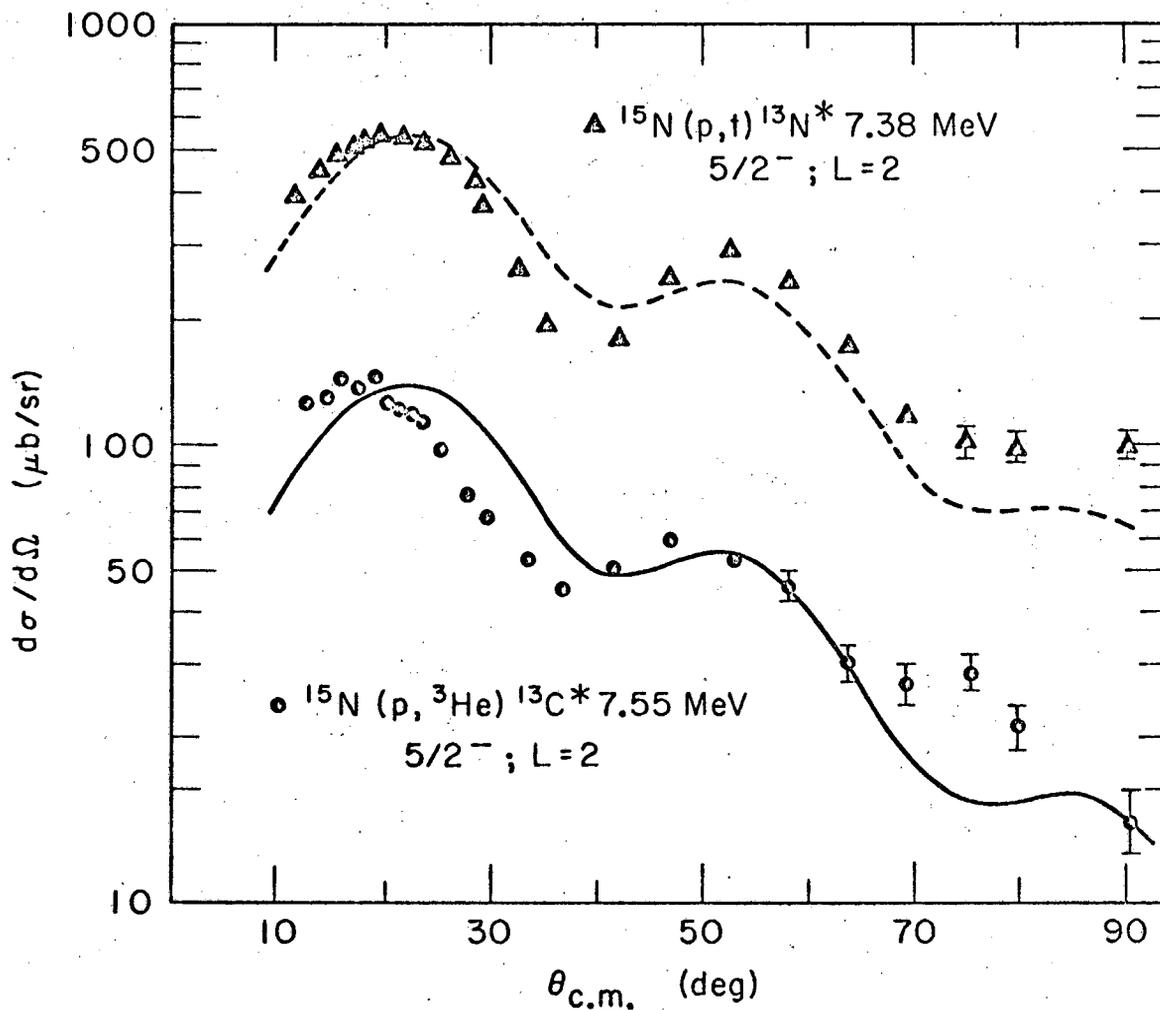
XBL676-3274-A

Fig. 19
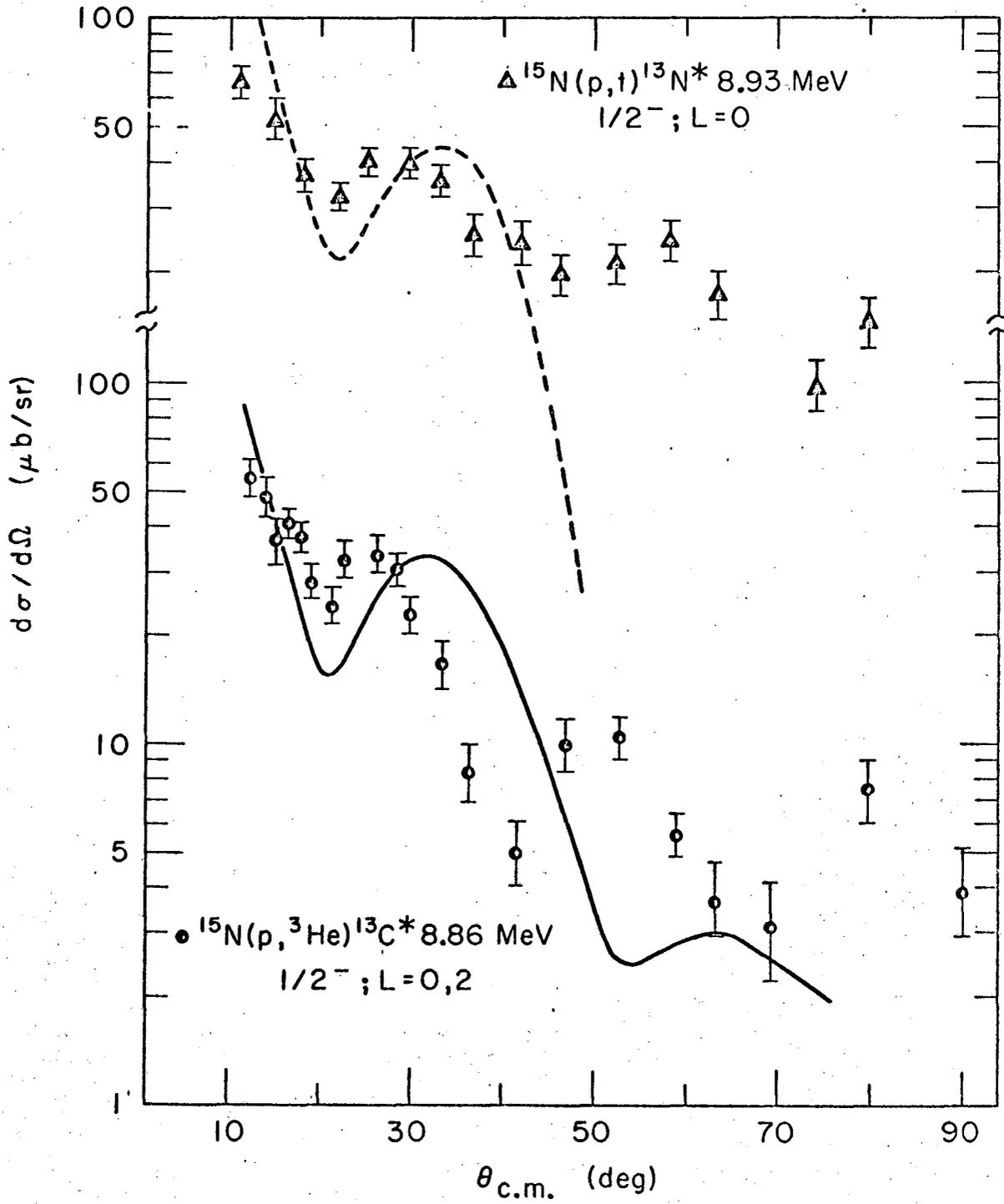
XBL 676-3281-A

Fig. 20
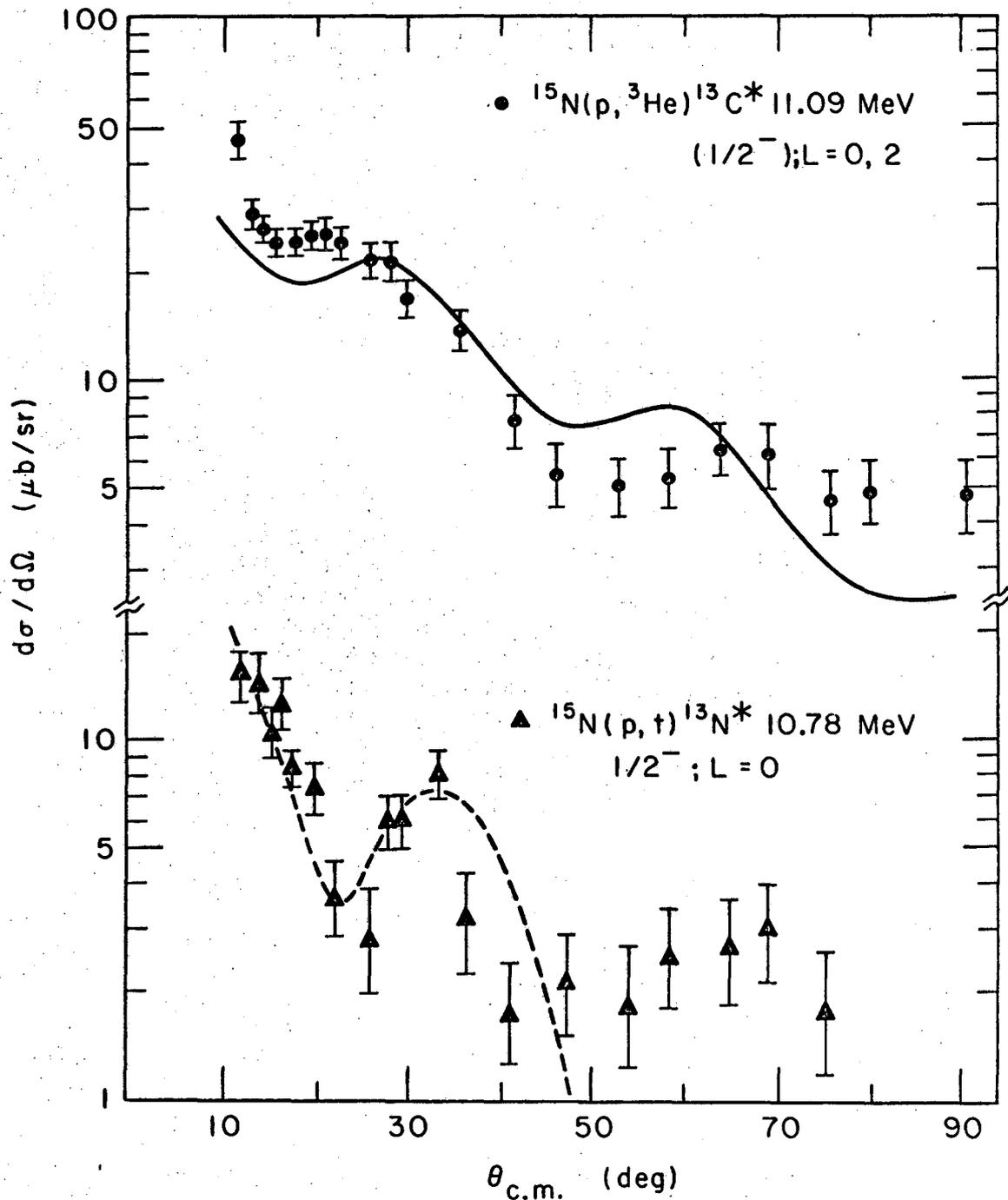
XBL676-3282A

Fig. 21

XBL676-3280-A

Fig. 22

$^{15}N(p,^{3}He)^{13}C^{*}$ 12.40 MeV
$7/2^{-}$; L=2

$\blacktriangle \, ^{15}N(p,t)^{13}N^{*}$ 15.07 MeV
$3/2^{-}$; T=3/2; L=2

$d\sigma/d\Omega$ $(\mu b/sr)$

$\theta_{c.m.}$ (deg)
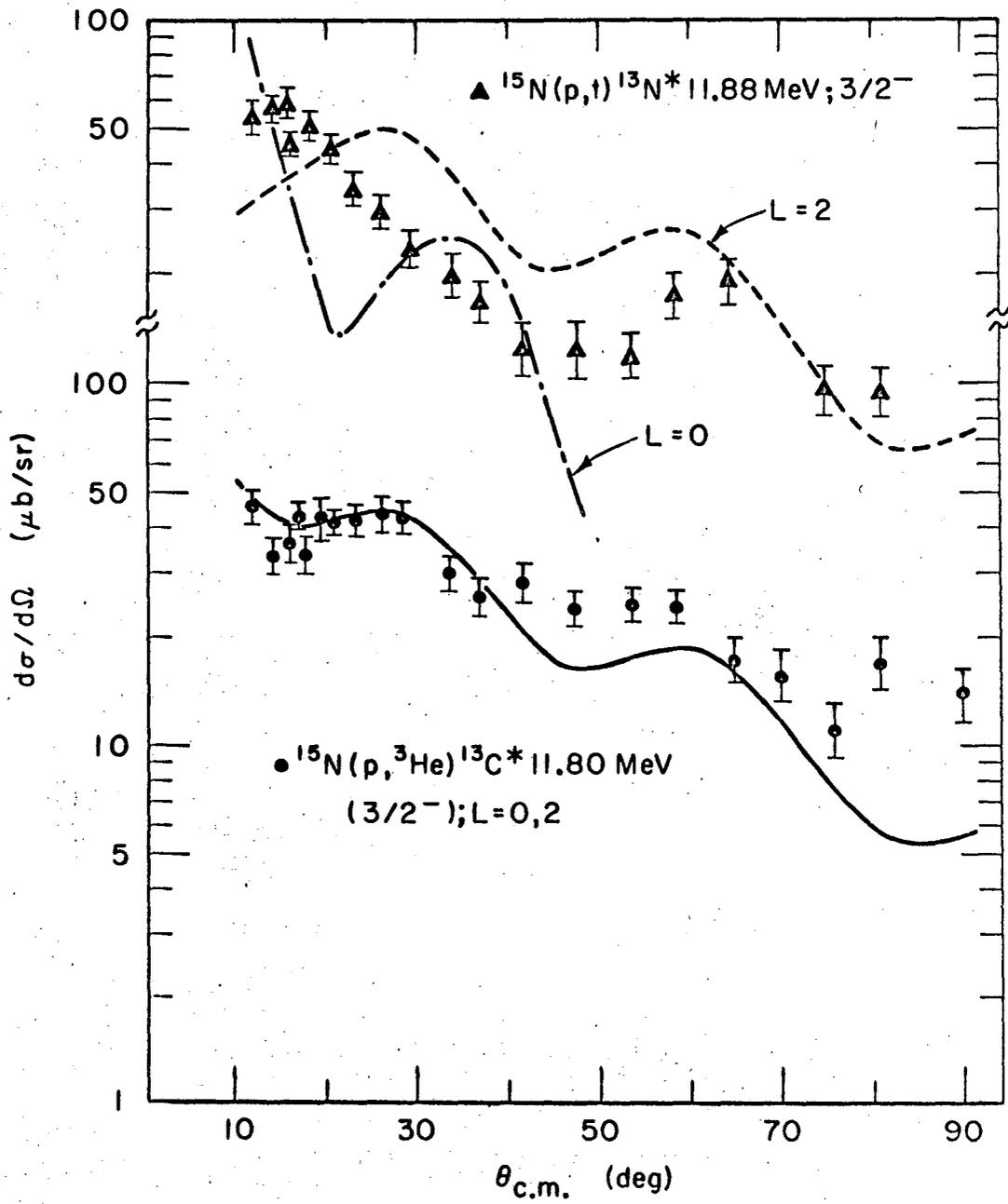
XBL 676-3283-A

Fig. 23

XBL 677-3547

Fig. 24